plants

MDPI

Article

Profiling Walnut Fungal Pathobiome Associated with Walnut Dieback Using Community-Targeted DNA Metabarcoding

Marie Belair, Flora Pensec, Jean-Luc Jany, Gaétan Le Floch and Adeline Picot *

Laboratoire Universitaire de Biodiversité et Ecologie Microbienne, INRAE, University Brest, F-29280 Plouzané, France

* Correspondence: adeline.picot@univ-brest.fr

Abstract: Walnut dieback can be caused by several fungal pathogenic species, which are associated with symptoms ranging from branch dieback to fruit necrosis and blight, challenging the one pathogen–one disease concept. Therefore, an accurate and extensive description of the walnut fungal pathobiome is crucial. To this end, DNA metabarcoding represents a powerful approach provided that bioinformatic pipelines are evaluated to avoid misinterpretation. In this context, this study aimed to determine (i) the performance of five primer pairs targeting the ITS region in amplifying genera of interest and estimating their relative abundance based on mock communities and (ii) the degree of taxonomic resolution using phylogenetic trees. Furthermore, our pipelines were also applied to DNA sequences from symptomatic walnut husks and twigs. Overall, our results showed that the ITS2 region was a better barcode than ITS1 and ITS, resulting in significantly higher sensitivity and/or similarity of composition values. The ITS3/ITS4_KYO1 primer set allowed to cover a wider range of fungal diversity, compared to the other primer sets also targeting the ITS2 region, namely, GTAA and GTAAm. Adding an extraction step to the ITS2 sequence influenced both positively and negatively the taxonomic resolution at the genus and species level, depending on the primer pair considered. Taken together, these results suggested that Kyo set without ITS2 extraction was the best pipeline to assess the broadest fungal diversity, with a more accurate taxonomic assignment, in walnut organs with dieback symptoms.

Keywords: metabarcoding; internal transcribed spacer (ITS); mock communities; environmental DNA (eDNA); walnut dieback; fungal pathogens

check for updates

Citation: Belair, M.; Pensec, F.; Jany, J.-L.; Le Floch, G.; Picot, A. Profiling Walnut Fungal Pathobiome Associated with Walnut Dieback Using Community-Targeted DNA Metabarcoding. *Plants* **2023**, *12*, 2383. https://doi.org/10.3390/plants12122383

Academic Editor: Hazem Salaheldin Elshafie

Received: 3 May 2023
Revised: 6 June 2023
Accepted: 12 June 2023
Published: 20 June 2023

1. Introduction

Walnut (*Juglans regia* L.) cultivation is one of the most important cultivations of nut crops worldwide, reaching more than 3.5 billion tons and 1.1 million hectares in 2021 [1]. China is the leading walnut producer, followed by the United States and Iran, while Europe ranks 5th [1]. Walnut orchards are usually affected by various pathogens, including *Xanthomonas campestris* pv. *juglandis*, which causes walnut blight, *Ophiognomonia leptostyla* and species from the *Colletotrichum acutatum* species complex, both responsible for walnut anthracnoses, as well as *Geosmithia morbida*, the causal agent of the "Thousand canker disease" [2–5]. Walnut dieback has also been frequently reported in California [6] as well as in Mediterranean-climate countries such as Spain [6,7], Italy [8], Turkey [9], and Czech Republic [10] over the past decade and more recently in France [11]. This fungal disease is characterized by symptoms such as fruit necrosis and blight, twig defoliation and dieback as well as branch canker up to host death [6–11]. The *Botryosphaeriaceae* family, mainly represented by the *Botryosphaeria*, *Diplodia* and *Neofusicoccum* genera, and *Diaporthe* spp. (teleomorph of *Phomopsis* spp.) were described as the causal agents in these countries; however, other pathogenic fungi such as *Colletotrichum* spp. and *Fusarium* spp. could be present in smaller proportions and participate in walnut decay and twig dieback [6,7,11–13]. Walnut dieback is thus likely to be caused by complexes of species working synergistically

and/or antagonistically to create, foster or mitigate disease onset and development as it has been demonstrated for dieback diseases affecting other tree crops such as vines [14]. As such, this disease is an excellent illustration of the pathobiome concept that can be defined as "the set of host-associated organisms associated with reduced (potentially reduced) health status, as a result of interactions between members of that set and the host" [15]. It is therefore important to investigate and thoroughly describe the fungal pathogens associated with these new symptoms in walnut orchards without neglecting the contribution of other members of the microbiota to disease development. To do so, environmental DNA (eDNA) metabarcoding represents a powerful culture-independent technique to decipher the mycobiota of affected walnut organs as well as their associations and thus gain access to the pathobiome functioning [16–20].

Metabarcoding has been extensively used to assess microbial diversity of various agroecosystems [21–24]. Recently, this method has been used to evaluate fungal diversity associated with leaves [25] and buds [5] of diseased walnut trees. Metabarcoding success and accuracy depend on the selection of the targeted region, the design of primer pairs, and the choice of adapted bioinformatic analysis pipelines [26–29]. It is then important to define an adapted and tailored analysis method for each ecosystem, considering the biases that may arise at each step of eDNA metabarcoding [26] from polymerase chain reaction (PCR) parameters and amplification [30–33] to taxonomic assignment of final reads during bioinformatic analysis [34]. The internal transcribed spacer (ITS) region is the universal barcode used to study fungal communities [35], and many studies have designed universal primers for the amplification of this region for a large number of fungal species [36–45].

In order to validate an analysis method, a mock community control is highly recommended [26,46]. It is composed of DNA solutions of known organisms, likely to be encountered in the targeted ecosystem, and mixed in known proportions. This positive control enables to evaluate and estimate numerous experimental, sequencing and bioinformatic analysis biases during sample preparation and DNA extraction, PCR sequence amplification (e.g., over- or under-representation of taxa and chimera formation), and taxonomic assignment [28,46–49].

To the best of our knowledge, our study is the first to validate metabarcoding protocols and assess fungal pathogen diversity associated with walnut diseases based on mock communities. The aim of this study was to define a metabarcoding methodology enabling the characterization of walnut fungal pathobiome associated with walnut dieback disease with an accurate taxonomic resolution up to the genus or species level. The validated method was subsequently applied on symptomatic husk and twig samples from walnut orchards.

2. Results

2.1. Analysis of Mock Communities and Identification of the Best Primer Sets

To evaluate the performance of each combination of primer pairs and pipelines in characterizing fungal mycobiota associated with symptomatic walnut organs, five mock communities, comprising between 5 to 18 fungal pathogenic and endophytic/saprophytic walnut-associated DNA species, were sequenced using Illumina MiSeq metabarcoding.

After read filtering, a total number of 3,509,971 sequence reads were obtained from 15 mock community samples (5 mocks × 3 replicates) and all primer pairs, with a mean number of sequences per sample ranging from 32,318 ± 5232 (GTAAm) to 78,792 ± 18,049 (Kyo) and a retention percentage of at least 41.6% after read trimming and filtering (Table S1). Rarefaction curves plotting the sequencing depth against the number of ASVs showed that the plateau phase was reached for every community and every primer set (Figure S1).

The distribution of genera showed a high repeatability between replicates irrespective of the mock and primer set (Figure 1). In addition, walnut DNA did not affect the quality of metabarcoding sequencing as shown by the similar distribution between Mock3 and Mock5 (Figure 1). Furthermore, similarity of composition values were not significantly different between these two mock communities ($p = 0.2997$, Kruskal-Wallis test).

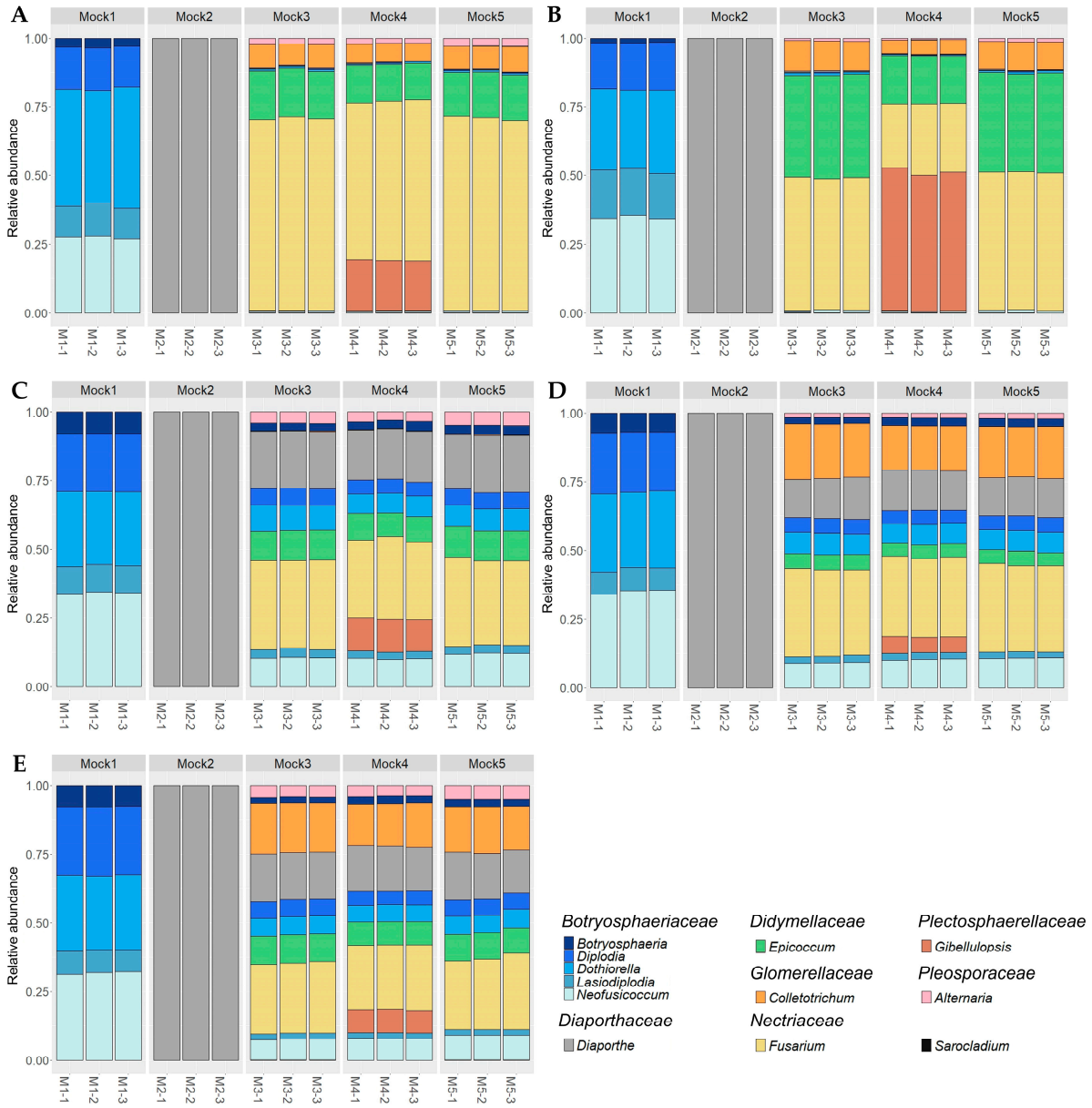

Figure 1. Histograms showing the relative abundance at the genus level for each replicate (−1, −2, −3) of mock communities (M1, M2, M3, M4, M5) according to metabarcoding sequencing based on the five primer sets: ITS (**A**), ITS1 (**B**), GTAA (**C**), GTAAm (**D**) and Kyo (**E**). Genera are ordered by family taxonomic rank in the legend. The *Sarocladium* genus is shown separately because it is not a component taxon of the mock communities and is identified as a contaminant genus.

All primer sets demonstrated the ability to detect *Botryosphaeriaceae* and *Diaporthe* species when these species were not mixed with others (Mock1 and Mock2) as shown by the high sensitivity values (Tables 1 and 2). However, they did not detect the complete diversity of Mock3, Mock4 and Mock5. The ITS1 primer set detected the lowest number of genera (up to 8 species out of 18 in at least one replicate of Mock4), and GTAA failed to amplify *Colletotrichum godetiae*, and its ability to detect *C. fioriniae* was relatively low (between 60 and 116 reads depending on replicate; Table 1). Moreover, considering the most diverse mock community (Mock4), no significant correlations were found between obtained and expected relative abundances for ITS (R = 0.012 and p = 0.95) and ITS1 sets (R = −0.17 and p = 0.35) mainly because of an overrepresentation of *Fusarium*, *Epicoccum* and *Gibellulopsis* genera and an underrepresentation of *Botryosphaeriaceae* and *Diaporthe* species (Figures 1 and 2).

Table 1. Genus recovery and primer sensitivity on mock communities. Cells were subdivided when results differed between replicates. Green cells correspond to True Positive (TP) ASVs (i.e., detected and well assigned at the genus level), blue and red cells to False Negative (FN) ASVs (i.e., detected but inaccurately assigned at the genus level, or not detected, respectively) and gray cells to species not involved in the mock community.

Fungal Species Included in Mock Communities	Mock1					Mock2					Mock3					Mock4					Mock5				
	ITS	ITS1	GTAA	GTAAm	Kyo	ITS	ITS1	GTAA	GTAAm	Kyo	ITS	ITS1	GTAA	GTAAm	Kyo	ITS	ITS1	GTAA	GTAAm	Kyo	ITS	ITS1	GTAA	GTAAm	Kyo
Botryosphaeria dothidea																									
Diplodia seriata																									
Dothiorella omnivora																									
Lasiodiplodia theobromae																									
Neofusicoccum mediterraneum																									
N. parvum																									
Diaporthe amygdali																									
Dia. eres																									
Dia. foeniculina																									
Dia. novem																									
Dia. rudis																									
Epicoccum nigrum																									
Colletotrichum fioriniae																									
C. godetiae																									
Fusarium juglandicola																									
F. solani																									
Gibellulopsis nigrescens																									
Alternaria alternata																									

Table 2. Sensitivity, precision and similarity of composition values and number of ASVs for each mock community and each primer pair. Results are presented as mean +/− standard deviation over the three technical replicates when they showed different values. ASVs assigned to *Sarocladium* were not taken into account for the calculation of the performance criteria.

Sample (Number of Expected ASVs)	Primer Set	Sensitivity	Precision	Similarity of Composition	Number of Obtained ASVs
Mock1 (6 ASVs)	ITS	0.833 ^{b}	0.045 ^{c} ± 0.001	0.739 ^{c} ± 0.016	113 ± 3.6
	ITS1	0.833 ^{b}	0.242 ^{abc} ± 0.007	0.845 ^{a} ± 0.003	21.7 ± 0.6
	GTAA	1 ^{a}	0.500 ^{a}	0.846 ^{ab} ± 0.001	12
	GTAAm	1 ^{a}	0.250 ^{ab}	0.820 ^{abc} ± 0.002	24
	Kyo	0.833 ^{b}	0.114 ^{bc}	0.814 ^{bc} ± 0.004	45
Mock2 (5 ASVs)	ITS	1 ^{a}	0.099 ^{b} ± 0.002	1 ^{a}	50.3 ± 1.1
	ITS1	1 ^{a}	0.341 ^{ac} ± 0.014	1 ^{a}	14.7 ± 0.6
	GTAA	1 ^{a}	0.500 ^{a}	1 ^{a}	10
	GTAAm	1 ^{a}	0.278 ^{abc}	1 ^{a}	18
	Kyo	1 ^{a}	0.135 ^{bc}	1 ^{a}	37
Mock3 (17 ASVs)	ITS	0.941 ^{a}	0.178 ^{ac} ± 0.003	0.301 ^{c} ± 0.007	90.7 ± 1.5
	ITS1	0.804 ^{b} ± 0.068	0.518 ^{b} ± 0.032	0.324 ^{ac} ± 0.005	27.3 ± 0.6
	GTAA	0.882 ^{ab}	0.454 ^{ab}	0.710 ^{ab} ± 0.003	34
	GTAAm	0.941 ^{a}	0.253 ^{abc} ± 0.002	0.702 ^{abc} ± 0.010	64.3 ± 0.6
	Kyo	0.882 ^{ab}	0.115 ^{c}	0.749 ^{b} ± 0.005	132
Mock4 (18 ASVs)	ITS	0.870 ^{b} ± 0.032	0.154 ^{b} ± 0.011	0.325 ^{ac} ± 0.003	103.7 ± 4.9
	ITS1	0.685 ^{b} ± 0.085	0.457 ^{a} ± 0.056	0.292 ^{c} ± 0.001	28
	GTAA	0.889 ^{ab}	0.453 ^{a} ± 0.015	0.707 ^{abc} ± 0.006	36.3 ± 1.1
	GTAAm	0.944 ^{a}	0.260 ^{ab} ± 0.002	0.751 ^{ab} ± 0.006	66.3 ± 0.6
	Kyo	0.889 ^{ab}	0.115 ^{b}	0.769 ^{b} ± 0.007	140.7 ± 0.6
Mock5 (17 ASVs)	ITS	0.941 ^{a}	0.178 ^{ac} ± 0.007	0.312 ^{c} ± 0.006	91 ± 3.5
	ITS1	0.706 ^{b} ± 0.059	0.495 ^{b} ± 0.025	0.327 ^{ac} ± 0.020	25.3 ± 3.0
	GTAA	0.882 ^{ab}	0.454 ^{ab}	0.731 ^{ab} ± 0.009	34
	GTAAm	0.941 ^{a}	0.255 ^{abc} ± 0.002	0.718 ^{abc} ± 0.005	63.7 ± 0.6
	Kyo	0.882 ^{ab}	0.117 ^{c} ± 0.004	0.764 ^{b} ± 0.009	129.7 ± 4.0

Lowercase letters indicate significant differences at 0.05 threshold based on Dunn's test. Statistical comparisons were performed by mock and by column.

Compared to ITS and ITS1 primer pairs, the three other sets targeting the ITS2 barcode showed overall better performance in terms of sensitivity and/or similarity of composition; however, Kyo was associated with the lowest precision values along with ITS. This discrepancy is mainly caused by metabarcoding sequencing with these primer pairs that generated supernumerary ASVs, thus overestimating the number of ASVs obtained compared to the expected number of ASVs and leading to low precision values at the ASV scale. First, GTAAm degenerated primer pair permitted the amplification and detection of *Colletotrichum* in addition to other genera of interest when compared with GTAA (Figure 1C,D). GTAAm was also associated with significantly higher sensitivity values than ITS1 when considering Mock4 (Table 2). Overall, both GTAAm and Kyo showed the highest positive and significant correlation coefficients between observed and expected relative abundances for Mock4 (R = 0.51; $p = 2.5 \times 10^{-3}$ and R = 0.6; $p = 2.4 \times 10^{-4}$ respectively; Figure 2). Nonetheless, both primer pairs underestimated or overestimated the relative abundance of a few studied genera. In particular, relative abundance of *Lasiodiplodia* was underestimated by both GTAAm and Kyo (with a ratio of expected to recovered relative abundances of 2.254 ± 0.079 and 2.603 ± 0.009, respectively) as well as the *Botryosphaeria* (1.838 ± 0.047 and 2.080 ± 0.058, respectively) and *Diaporthe* relative abundances (1.908 ± 0.041 and 1.711 ± 0.050, respectively). *Alternaria* was underestimated by GTAAm (3.183 ± 0.146),

and *Fusarium* was overestimated by both GTAAm (0.383 ± 0.003) and Kyo (0.468 ± 0.005; Figures 1 and 2).

Given that GTAA failed to amplify *Colletotrichum* species, which are important pathogens of interest in walnut, while ITS and ITS1 provided poor similarity of composition values, only GTAAm and Kyo were utilized for the following steps, i.e., optimization of bioinformatic analyses and analysis of environmental samples.

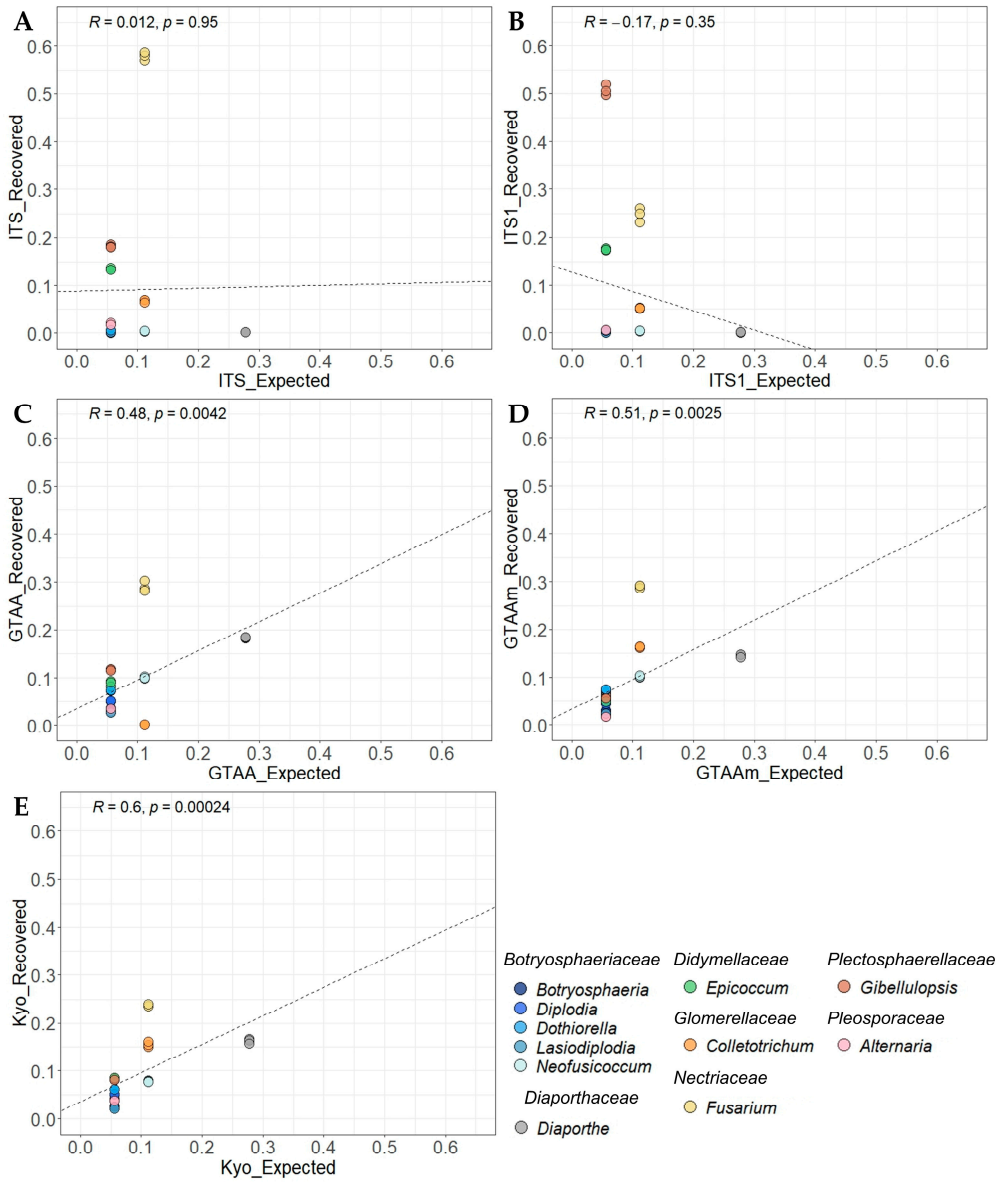

Figure 2. Recovered relative abundances plotted against expected ones at the genus level obtained for Mock4 for each primer set: ITS (**A**), ITS1 (**B**), GTAA (**C**), GTAAm (**D**) and Kyo (**E**). Pearson's correlation coefficients were calculated based on the relative abundance values of the three replicates.

2.2. Evaluation of the Taxonomic-Level Resolution

The genus- and species-level resolution of regions targeted by GTAAm and Kyo was assessed using phylogenetic trees based on ITS2 sequences of wood and fruit-associated pathogens.

First, phylogenetic trees with Bayesian posterior probabilities (BPP) were constructed based on our local amplicon databases, subjected or not to an extraction of the ITS2 region, in order to evaluate the impact of an extraction step with ITSx software on the quality of taxonomic resolution. Taxonomy of the fungal species included in mock communities was

manually inspected and validated up to the species or genus level if nodes before clade containing targeted species or genus were supported by relatively strong BPP values (>0.70, considering that the analysis is based only on 1 locus; Table 3). At the species level, the highest assignment rates with both primer pairs were obtained without ITS2 extraction for Kyo (9 out of 18 species included in mock communities) and with ITS2 extraction for GTAAm (5 out of 18; Table 3). The main issues resulted from a few *Dothiorella* species and *N. mediterraneum* that were clustered together (in all conditions), *N. parvum* that was often clustered with the previous ones (except for Kyo without ITSx extraction condition) and *B. dothidea* that could not be differentiated from *Neoscytalidium dimidiatum* in most conditions (except for GTAAm with ITSx extraction condition; Table 3). These species were therefore given new assignments considering their possible multiple assignments (e.g., *N. parvum* was reassigned as *Neofusicoccum/Dothiorella* and *B. dothidea* as *Botryosphaeria/Neoscytalidium* for the relevant conditions). Moreover, *L. theobromae* sequences were always mixed with other *Lasiodiplodia* species, while *F. juglandicola* sequences were mixed with *F. avenaceum* ones.

Table 3. Determination of the genus- and species-level resolutions obtained with GTAAm and Kyo with (w/) or without (wo/) ITSx extraction after DADA2 sequence pre-processing and following validation of taxonomic assignment with phylogenetic trees. Green cells correspond to a correct assignment at the genus or species level, blue cells correspond to an inaccurate assignment and gray cells to fungal species absent from our local databases.

Fungal Species Included in Mock Communities	GTAAm				Kyo			
	w/		wo/		w/		wo/	
	Genus	Species	Genus	Species	Genus	Species	Genus	Species
Botryosphaeria dothidea								
Diplodia seriata								
Dothiorella omnivora								
Lasiodiplodia theobromae								
Neofusicoccum mediterraneum								
N. parvum								
Diaporthe amygdali								
Dia. eres								
Dia. foeniculina								
Dia. novem								
Dia. rudis								
Epicoccum nigrum								
Colletotrichum fioriniae								
C. godetiae								
Fusarium juglandicola								
F. solani								
Gibellulopsis nigrescens								
Alternaria alternata								

Second, additional phylogenetic trees were built by adding ASVs sequences (from metabarcoding of mock samples) to our local database to determine their taxonomic placement within the tree and whether it was in accordance with their assignment after a blast against our ITS local database. We found that ASVs were generally grouped with the corresponding reference sequences at the genus or species level, regardless of the combination of primer pairs and pipelines (Figure 3).

The manually-corrected taxonomy of ASVs, as described above, was also used to compare the performance criteria of the two selected primer pairs depending on the addition of an extraction step of the ITS2 sequence. This step did not affect the mean number of reads after filtering for all mock communities for the two primer pairs, suggesting that no aspecific amplifications occurred (Table S1). Thus, the average number of ASVs using mock community remained the same as well as the similarity of composition at the genus and species level, which was significantly higher with Kyo for Mock3 to Mock5 (Table 4).

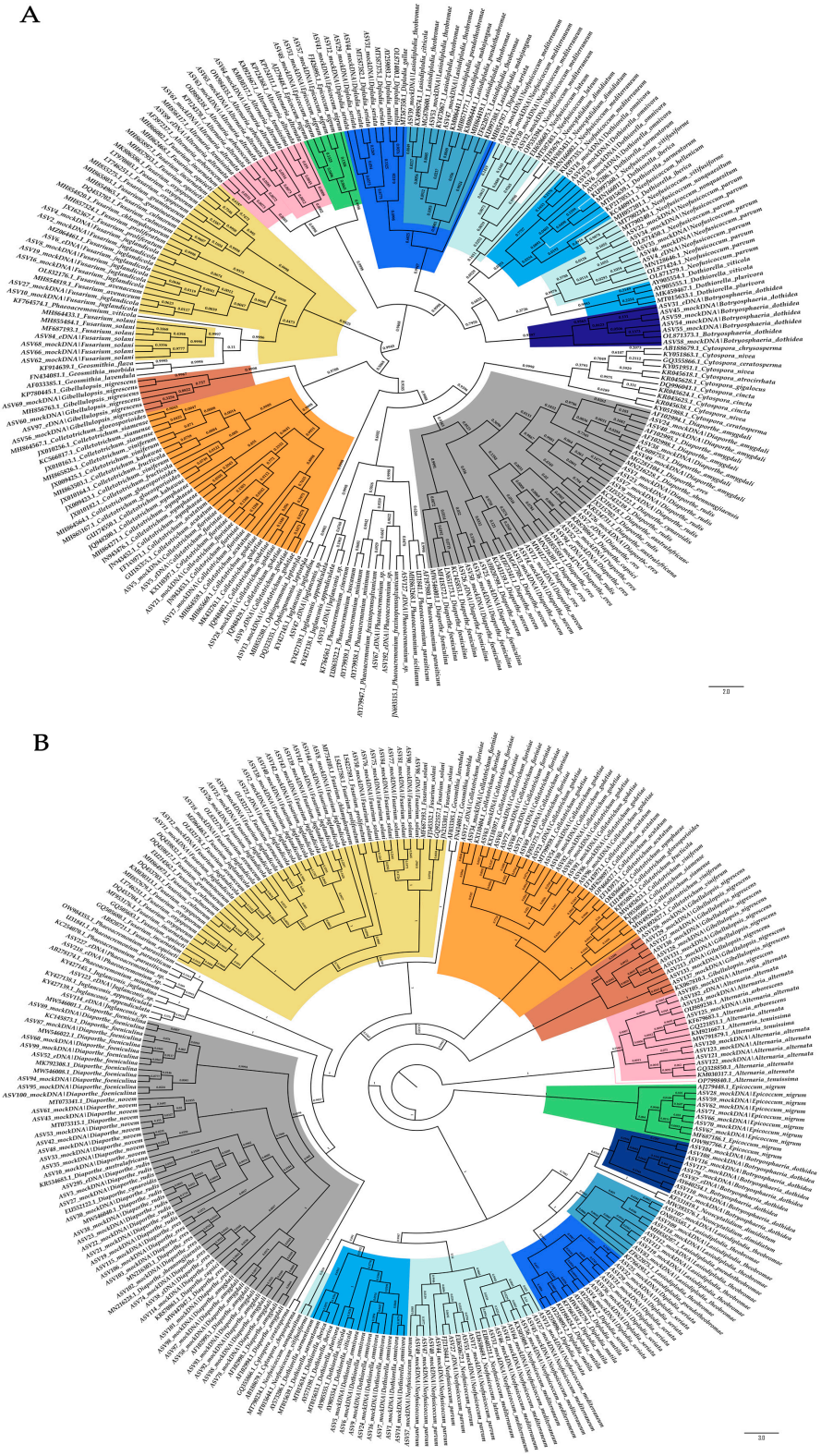

Figure 3. Bayesian inference phylogenetic consensus cladogram gathering ASVs from mock communities (mockDNA) and from environmental samples (eDNA) obtained from metabarcoding sequencing with GTAAm with ITSx extraction (**A**) and Kyo without ITSx extraction (**B**). Bayesian posterior probabilities values are represented at branches. Taxonomic assignment of ASVs from mock communities was based on the local ITS database, and taxonomic assignment of supplementary environmental ASVs (i.e., for *Juglanconis* and *Phaeoacremonium* genera) was based on BLASTn results. Phylogenetic cladograms were rooted with *Alternaria*.

Table 4. Sensitivity, precision and similarity of composition values for GTAA182f/GTAA526r (GTAAm) and ITS3/ITS4_KYO1 (Kyo) primer pairs with (w/) or without (w/o) ITS2 extraction at the genus (Gen) and species level (Sp) after manual inspection of taxonomic assignment. Results are presented as mean +/− standard deviation over the three replicates. ASVs assigned to *Sarocladium* were not taken into account for the calculation of the performance criteria.

Sample	Primer Set	Sensitivity				Precision				Similarity of Composition	
		Genus		Species		Genus		Species			
		w/	w/o	w/	w/o	w/	w/o	w/	w/o	Genus	Species
Mock1	GTAAm	0.5^{a}	0.333^{b}	0.167^{a}	0^{b}	0.143^{a}	0.1^{ab}	0.053^{a}	0^{b}	$0.820^{A} \pm 0.002$	$0.822^{A} \pm 0.004$
	Kyo	0.333^{b}	0.5^{a}	0.167^{a}	0.167^{a}	0.049^{c}	0.071^{bc}	0.025^{ab}	0.025^{ab}	$0.814^{B} \pm 0.004$	$0.826^{A} \pm 0.006$
Mock2	GTAAm	1^{a}	1^{a}	0.4^{a}	0.4^{a}	0.278^{a}	0.278^{a}	0.133^{a}	0.133^{a}	1^{A}	$0.790^{A} \pm 0.004$
	Kyo	1^{a}	1^{a}	0.5^{a}	0.6^{b}	0.135^{b}	0.135^{b}	0.059^{b}	0.086^{ab}	1^{A}	$0.817^{B} \pm 0.004$
Mock3	GTAAm	0.823^{a}	0.765^{b}	0.235^{ab}	0.176^{a}	$0.228^{a} \pm 0.002$	$0.215^{ab} \pm 0.002$	$0.078^{a} \pm 0.001$	$0.060^{bc} \pm 0.001$	$0.702^{A} \pm 0.010$	$0.655^{A} \pm 0.008$
	Kyo	0.765^{b}	0.823^{a}	0.236^{ab}	0.470^{b}	0.101^{c}	0.108^{bc}	0.034^{b}	0.065^{ac}	$0.749^{B} \pm 0.005$	$0.745^{B} \pm 0.001$
Mock4	GTAAm	0.833^{a}	0.779^{b}	0.278^{ab}	0.222^{a}	$0.237^{a} \pm 0.002$	$0.225^{ab} \pm 0.002$	$0.094^{a} \pm 0.001$	$0.076^{ab} \pm 0.001$	$0.751^{A} \pm 0.006$	$0.710^{A} \pm 0.003$
	Kyo	0.778^{b}	0.833^{a}	0.245^{ab}	0.5^{b}	0.102^{c}	0.109^{bc}	0.039^{c}	0.068^{bc}	$0.769^{B} \pm 0.007$	$0.770^{B} \pm 0.008$
Mock5	GTAAm	0.823^{a}	0.765^{b}	0.235^{ab}	0.176^{a}	0.229^{a}	$0.219^{ab} \pm 0.002$	0.078^{a}	$0.060^{bc} \pm 0.001$	$0.718^{A} \pm 0.005$	$0.672^{A} \pm 0.004$
	Kyo	0.765^{b}	0.823^{a}	0.235^{ab}	0.470^{b}	$0.103^{c} \pm 0.003$	$0.111^{bc} \pm 0.003$	$0.034^{b} \pm 0.001$	$0.066^{ac} \pm 0.002$	$0.764^{B} \pm 0.009$	$0.765^{B} \pm 0.010$

w/: with ITSx extraction; w/o: without ITSx extraction; Genus: genus level; Species: species level. Lowercase letters indicate significant differences at 0.05 threshold based on Dunn's test. Statistical comparisons were performed by level (genus or species) between primer sets for sensitivity and precision values with and without ITSx extraction for each mock community. Uppercase letters indicate significant differences at 0.05 threshold based on Wilcoxon's test. Statistical comparisons were performed by level (genus or species) and by mock between primer sets for compositional similarity values.

In contrast, sensitivity at the genus level was significantly higher with GTAAm than with Kyo when a step of ITS2 extraction was added, while the opposite was found without the ITS2 extraction step (Table 4). In any case, at the species level, the highest sensitivity rate was obtained with Kyo without ITS2 extraction, further confirming that these conditions were the best to correctly assign the fungi of interest at this taxonomic rank (Table 4). Nonetheless, the precision criterion at the genus level remained significantly higher with GTAAm with ITS2 extraction than with Kyo (with ($p = 3.2 \times 10^{-4}$) and without ($p = 0.008$) ITS2 extraction).

2.3. Application on Environmental Samples

Based on these results, the two combinations GTAAm with ITS2 extraction and Kyo without ITS2 extraction were then applied on symptomatic environmental samples. The samples were collected from three French walnut orchards (P7, P10 and P12) and matched with symptomatic twigs (T) or husks (H). Taxonomic assignment of ASVs corresponding to phytopathogenic fungi of interest (i.e., fungal taxa introduced in mock communities) was manually inspected and modified as described above. Taxonomic assignment of the other fungal taxa was manually corrected at the genus level, or family level when necessary, based on the first 150 hits obtained with BLASTn.

After read filtering, ITS2 metabarcoding sequencing of the three replicates of six walnut samples yielded a total of 1,151,054 read sequences with Kyo (63,947 ± 33,362 mean reads per sample clustered into 108 ± 23 ASVs), while 693,700 read sequences (38,539 ± 10,832 mean reads per sample clustered into 49 ± 17 ASVs) were obtained with GTAAm. Replicate P7-H-2020-3 was associated with only 173 raw sequence reads when amplified with GTAAm and was discarded from further analysis. Combining results from husks and twigs, 25 and 24 genera were obtained for GTAAm and Kyo, respectively, of which 18 were in common. Each combination of primer pair and pipeline enabled the detection of the pathogenic genera in walnut trees, i.e., *Botryosphaeria/Neoscytalidium*, *Neofusicoccum/Dothiorella*, *Colletotrichum*, *Diaporthe*, *Fusarium*, *Juglanconis* and *Phaeoacremonium* (Figures 3 and 4). Unlike Kyo, GTAAm did not permit the detection of *Epicoccum* genus as well as *Basidiomycota* taxa (*Bulleribasidiaceae* family mainly represented by *Vishniacozyma* genus and to a lesser extent unidentified genera of *Sirobasidiaceae* family and *Tremellales* order). Moreover, Kyo showed a better taxonomic resolution for certain genera within the *Pleosporales* order than GTAAm. The genera *Angustimassarina* and *Biatriospora* were

identified with Kyo but were reassigned at the order level (unidentified_*Pleosporales*) with GTAAm (Figure 4).

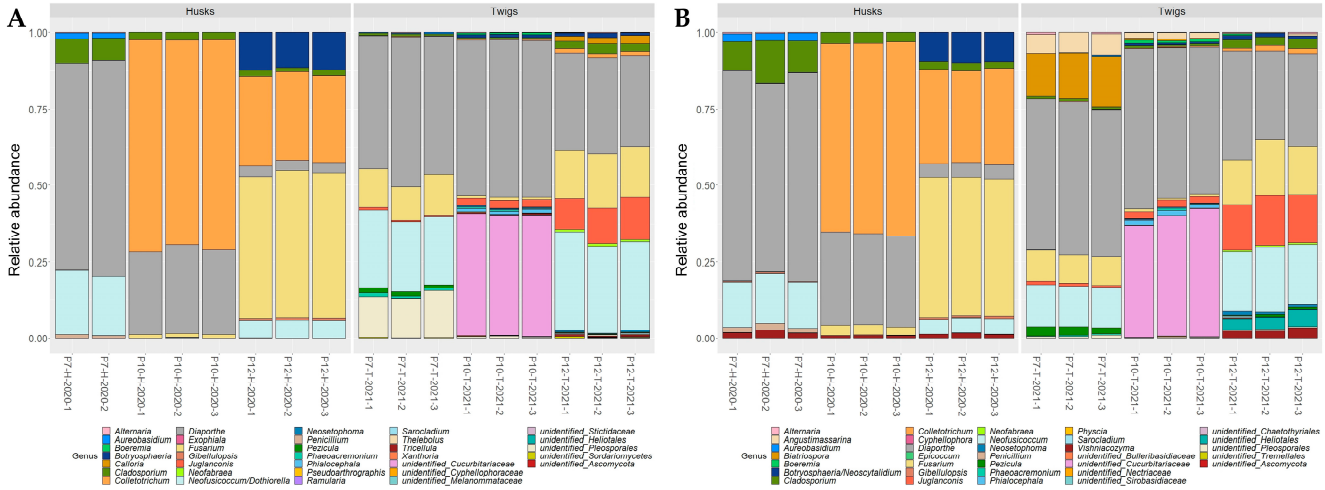

Figure 4. Histograms showing the relative abundance of fungal genera in environmental samples collected in 2020 and 2021 in replicates (−1, −2, −3) of walnut husks (H) and twigs (T) from three orchards (P7, P10, P12). Relative abundances were obtained with metabarcoding sequencing after amplification with GTAAm with ITS2 region extraction (**A**) and Kyo without ITS2 region extraction (**B**).

For both primer sets, alpha-diversity indices, including Shannon and InvSimpson indices calculated at the genus level, were not significantly different irrespective of the index and the type of organ studied. Nonetheless, the number of detected genera (observed index) associated with environmental husk samples was significantly higher with Kyo than with GTAAm, further highlighting a better capacity of Kyo to cover a wider range of diversity ($p = 0.004$; Figure 5).

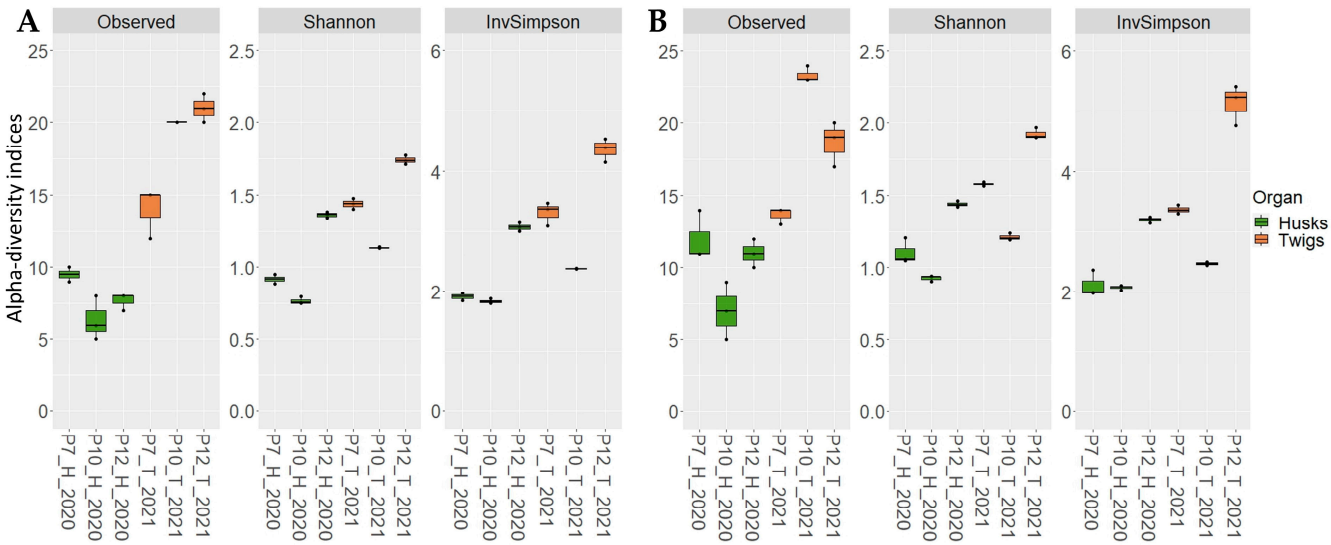

Figure 5. Alpha-diversity indices calculated at the genus level on the rarefied dataset in environmental samples (Husks: H and Twigs: T) from three orchards (P7, P10 and P12) obtained with GTAAm (**A**) and Kyo (**B**) combinations.

3. Discussion

The aim of this study was to define both metabarcoding parameters and bioinformatic pipeline to profile the fungal pathobiome associated with walnut dieback symptoms in eDNA samples. In order to choose the best combination of barcode and pipeline, we assessed the ability of five primer pairs to detect, assign and accurately estimate the relative abundance of fungal strains commonly associated with walnut or walnut dieback included in mock communities using Illumina MiSeq PE 300 bp sequencing. The selection of targeted barcodes, primers and bioinformatic pipelines is crucial in light of their significant influence on the resolution of taxonomic assignment [29,50–53]. The five primer pairs, all targeting whole or a part of the ITS region designated as the fungal universal barcode [35], i.e., ITS1, ITS2 and ITS, were compared using the DADA2 bioinformatic tool. Here, targeting the ITS2 region was shown to improve similarity of composition and/or sensitivity compared to ITS and ITS1. In addition, the quality of the analysis also depends largely on bioinformatic pipelines that must be tailored according to the fungal taxa expected to be associated with the considered ecosystem. Many studies have compared various barcodes for optimal fungal community analyses, which evidenced a lack of consensus in the choice of the best barcode between ITS1, ITS2 or the whole ITS region probably because it notably depends on the fungal taxa that are being considered [20,54–58]. For instance, the GTAA primer pair was set aside in this study because of its inability to amplify *Colletotrichum* species, which were not part of the tested fungal species by Morales-Cruz et al. [20]. The degeneration of the forward primer of this barcode enabled to solve this issue as suggested by Tedersoo et al. (2016) to minimize primer bias [29].

Interestingly, two primer pairs targeting the ITS2 region, GTAA182fm/GTAA526r and ITS3/ITS4_KYO1, provided the most accurate identifications and estimations of relative abundances and were selected for further analyses. On the basis of phylogenetic trees, both sets showed the same overall ability in distinguishing fungi of interest at the genus level, while Kyo showed better taxonomic resolution at the species level without the use of ITSx. This manual inspection step showed that care should be taken with the ASVs assignment just after bioinformatic pre-processing as it strongly depends on the taxonomic assignment algorithm as well as on the database even when UNITE database, the largest curated database dedicated to ITS sequences, is used [53,59]. Note that the same analyses were performed with the UNITE+INSDC non-redundant fungal ITS database v8.3 (1,039,010 ITS fungal sequences) before the latest version was released. The accuracy of the taxonomic assignment was much lower than those obtained with the v9.0 database (6,441,764 ITS fungal sequences). Thus, the number of sequences in the database, the diversity it covers, and the quality of the sequences are other crucial parameters in the quality of metabarcoding sequencing bioinformatic analyses [60–62]. The use of the latest version of a reference database seems to be essential, especially in view of the increase of knowledge about microbial diversity and of available sequences. The manual curation step allowed for the reassignment of ASVs to a more rightful taxonomic rank, notably those initially assigned to *Botryosphaeria dothidea* and *Neofusicoccum* spp. that were found clustered with a few other genera in the phylogenetic tree and therefore reassigned accordingly (Table 3).

Although Kyo and GTAAm provided high similarity of composition values, there were a few discrepancies between expected and observed relative abundances, up to a factor of 3. This has been consistently reported in many studies, and it was hypothesized that ITS length polymorphism likely accounted for such differences [63,64]. In other words, shorter amplicons are more likely to amplify during PCR [65] resulting in overrepresented taxa and, consequently, due to the compositional nature of metabarcoding data, underrepresented taxa [66]. Additional polymorphism form that could lead to an overestimation of taxa is the copy number variation (CNV) of the targeted region. Recently, Lofgren et al. (2019) inferred using in silico analysis of fungal genomes that the CNV of ribosomal DNA containing the ITS region could vary from 14 to 1442 copies among 91 fungal taxa belonging to *Ascomycota*, *Basidiomycota*, *Chytridiomycota*, *Mucoromycota* and *Zoopagomycota* phyla [67]. Another main bias associated with PCR is that more abundant taxa are more likely to be

amplified [66], which was actually not evaluated in our mock communities mixed in even proportions. Nanopore and PacBio sequencing technologies do not require a PCR step and may thus overcome these issues. In addition, sequencing longer reads allow a more accurate taxonomic assignment. However, the use of these technologies are still limited probably because of their high cost.

Furthermore, extraction of the variable ITS1 or ITS2 regions from raw sequences is recommended in many pipelines in order to discard conserved flanking sequences and thus improve species identification [51,68,69]. Based on this study, the interest of adding an extraction step depended on the primer set tested. Actually, extraction of the ITS2 region improved sensitivity with GTAAm, while the opposite was found with Kyo, and most probably was because of the loss of genetic information in sequences obtained with Kyo in the 28S region. Finally, we evaluated the capacity of the combinations of the two selected primer pairs with and without ITS2 extraction to describe well the symptomatic environmental samples. All conditions tested successfully permitted the detection and amplification of the major fungal phytopathogens and endophytes or saprophytes associated with walnut dieback and trunk diseases worldwide, namely, *Botryosphaeria*, *Colletotrichum*, *Diaporthe*, *Fusarium*, *Neofusicoccum*, *Juglanconis* and *Phaeoacremonium* genera [5,10,25,70–72]. Alpha-diversity indices were not significantly different between the two primer pairs except for the number of detected genera associated with walnut husk samples, which was significantly higher with Kyo. Note that only Kyo led to the amplification of *Basidiomycota* sequences, providing a broader view of fungal diversity of the pathobiome in the environmental samples [38].

4. Materials and Methods

4.1. Identification of Primer Sets Targeting Walnut Pathogens

The internal transcribed spacer (ITS) of the ribosomal DNA region was chosen as target barcode to identify fungal communities. A local database was built with full length ITS sequences of 78 species from 17 genera commonly isolated from walnut, almond, pistachio and olive trees worldwide, i.e., *Geosmithia, Botryosphaeria, Diplodia, Dothiorella*, *Lasiodiplodia*, *Neofusicoccum*, *Neoscytalidium*, *Diaporthe*, *Epicoccum*, *Colletotrichum*, *Ophiognomonia*, *Juglanconis, Fusarium*, *Gibellulopsis*, *Alternaria*, *Phaeoacremonium* and *Cytospora* (Table 5). The database was generated by downloading ITS sequences from the Genbank database [73] of National Center for Biotechnology Information [74] (accessed on 21 May 2021) for each fungal species using the query word 'internal transcribed spacer'. Up to 10 sequences per species were retrieved as well as the species reference sequence (RefSeq) when available [75].

Three universal primer sets amplifying the whole ITS region (ITS1F/ITS4, hereafter ITS [36,37]), the ITS1 region (ITS1F/ITS2, hereafter ITS1 [36,37]) and the ITS2 region (ITS3/ITS4_KYO1, hereafter Kyo [36,38]) regions were selected. Two primer sets were added because of their ability to specifically amplify part of the pathogens of interest (GTAA182f/526r and GTAA182fm/526r, hereafter GTAA and GTAAm, respectively) (Table 6 and Figure 6). GTAA was designed by Morales-Cruz et al. [20] to amplify grapevine-associated pathogens using metabarcoding sequencing, and some of which are common to those isolated from nut crops (i.e., *Botryosphaeria*, *Diplodia*, *Dothiorella*, *Lasiodiplodia*, *Neofusicoccum*, *Diaporthe* and *Phaeoacremonium*). In silico amplification of the local ITS database with the GTAA182f/526r primer pair was performed using Geneious Prime 2021.1.1 (settings: pairs only anywhere on the sequences and two mismatches allowed except within 15 bp of 3′ end; https://www.geneious.com (accessed on 21 May 2021). Since primers GTAA182f/526r failed to amplify the targeted region in *Colletotrichum* spp. because of a mismatch in the forward primer sequence, it was modified by replacing the C base in the 9th position by Y and renamed GTAA182fm.

Table 5. Fungal species associated with wood and fruit diseases among nut and olive trees.

Classification	Species	Host (Species)				References
		Walnut (*Juglans regia*)	Almond (*Prunus dulcis*)	Pistachio (*Pistacia vera*)	Olive (*Olea europaea*)	
Bionectriaceae	*Geosmithia flava*			X		[76]
	G. lavendula			X		[76]
	G. morbida	X				[77,78]
Botryosphaeriaceae	*Botryosphaeria dothidea*	X	X	X	X	[11,12,79–85]
	Diplodia gallae	X				[70]
	D. mutila	X	X	X	X	[80,83,84,86–88]
	D. seriata	X	X	X	X	[7,80–83,86,87,89–91]
	Dothiorella iberica	X	X	X	X	[80,83,87,91]
	Dot. omnivora	X				[10,70]
	Dot. plurivora	X				[70]
	Dot. sarmentorum	X	X	X		[7,70,81,91]
	Dot. viticola	X	X			[70,87]
	Lasiodiplodia citricola	X		X		[70,80,91]
	L. mahajangana	X		X		[70,92]
	L. pseudotheobromae	X		X		[85,93]
	L. theobromae	X	X	X	X	[70,81,83,84,87]
	Neofusicoccum hellenicum			X		[92]
	N. luteum				X	[83,84]
	N. mediterraneum	X	X	X	X	[7,80,81,83,85,87,88,91]
	N. nonquaesitum	X	X			[80,81]
	N. parvum	X	X	X	X	[7,11,80–82,84–87]
	N. vitifusiforme	X	X	X	X	[80,83,87,90,91]
	Neoscytalidium dimidiatum	X	X	X	X	[80,87,94–96]
Diaporthaceae	*Diaporthe amygdali*	X	X			[7,82,97,98]
	Dia. australafricana	X	X			[86,87]
	Dia. biguttulata	X				[99]
	Dia. capsici	X				[100]
	Dia. cynaroidis	X				[86]
	Dia. eres	X	X			[10,11,87,99]
	Dia. foeniculina	X	X	X	X	[7,11,80,85,90,98]
	Dia. juglandicola	X				[101]
	Dia. novem	X	X			[87], this study
	Dia. rudis	X		X	X	[83,91,102], this study
	Dia. shennongjiaensis	X				[103]
Didymellaceae	*Epicoccum nigrum*	X			X	[11,84]
Glomerellaceae	*Colletotrichum acutatum*	X	X	X	X	[104–108]
	C. fioriniae	X	X	X	X	[5,11,105,107,109–111]
	C. fructicola	X				[112]
	C. gloeosporioides	X		X	X	[5,107,109,113,114]
	C. godetiae	X	X		X	[5,11,106,107,109,110]
	C. kahawae	X			X	[109,114]
	C. nymphaeae	X	X		X	[5,109,115–117]
	C. siamense	X		X	X	[108,113,114]
	C. viniferum	X				[104]
Gnomoniaceae	*Ophiognomonia leptostyla*	X				[118,119]
Juglanconidaceae	*Juglanconis appendiculata*	X				[71]
	J. juglandina	X				[71,120]
Nectriaceae	*Fusarium avenaceum*	X	X	X		[121–125]
	F. chlamydosporum			X	X	[125,126]
	F. culmorum	X		X		[121,123,125]
	F. equiseti			X		[125]
	F. graminearum	X				[123]
	F. incarnatum	X		X		[123,125,127]
	F. juglandicola	X				[128]
	F. oxysporum	X		X	X	[121,123,125,126]
	F. proliferatum	X		X		[123,129]
	F. solani	X	X	X	X	[11,124–126,130,131]
Plectosphaerellaceae	*Gibellulopsis nigrescens*	X				[11]
Pleosporaceae	*Alternaria alternata*	X	X	X	X	[79,84,121,132,133]
	A. arborescens		X	X		[132,133]
	A. tenuissima	X	X	X	X	[79,84,130,132,133]

Table 5. *Cont.*

Classification	Species	Host (Species)				References
		Walnut (*Juglans regia*)	Almond (*Prunus dulcis*)	Pistachio (*Pistacia vera*)	Olive (*Olea europaea*)	
Togniniaceae	*Phaeoacremonium cinereum*	X		X		[70]
	P. fraxinopennsylvanicum	X				[70]
	P. italicum	X	X		X	[70,134]
	P. minimum	X	X	X	X	[70,85,90]
	P. parasiticum	X	X	X	X	[70,90,134]
	P. sicilianum	X			X	[10,134]
	P. tuscanum	X				[70]
	P. viticola	X	X	X	X	[70,135]
Valsaceae	*Cytospora atrocirrhata*	X				[136,137]
	Cyt. californica	X	X	X		[87,88,136]
	Cyt. ceratosperma	X				[137]
	Cyt. chrysosperma	X				[136,138]
	Cyt. cincta	X				[138]
	Cyt. gigalocus	X				[136,137]
	Cyt. joaquinensis	X		X		[88,136]
	Cyt. nivea	X				[139]
	Cyt. plurivora	X	X	X	X	[87,136]

Table 6. Summary of PCR primers used in this study for metabarcoding sequencing. Amplicon sizes are based on the ITS region of *N. parvum* (OL639139.1) presented in Figure 1.

Barcode	Primer Name	Set Name	Direction	Sequence (5′-3′)	Amplicon Size (bp)	Primer Reference
ITS	ITS1F ITS4	ITS	Forward Reverse	CTTGGTCATTTAGAGGAAGTAA TCCTCCGCTTATTGATATGC	617	[37] [36]
ITS1	ITS1F ITS2	ITS1	Forward Reverse	CTTGGTCATTTAGAGGAAGTAA GCTGCGTTCTTCATCGATGC	295	[37] [36]
ITS2	GTAA182f GTAA526r	GTAA	Forward Reverse	AAAACTTTCAACAACGGATC TYCCTACCTGATCCGAGGTC	337	[20] [20]
	GTAA182fm GTAA526r	GTAAm	Forward Reverse	AAAACTTTYAACAACGGATC TYCCTACCTGATCCGAGGTC	337	This study [20]
	ITS3 ITS4_KYO1	Kyo	Forward Reverse	GCATCGATGAAGAACGCAGC TCCTCCGCTTWTTGWTWTGC	342	[36] [38]

In bold, the two primer pairs selected to compare the performance of taxonomic assignment and applied to metabarcoding sequencing of environmental samples.

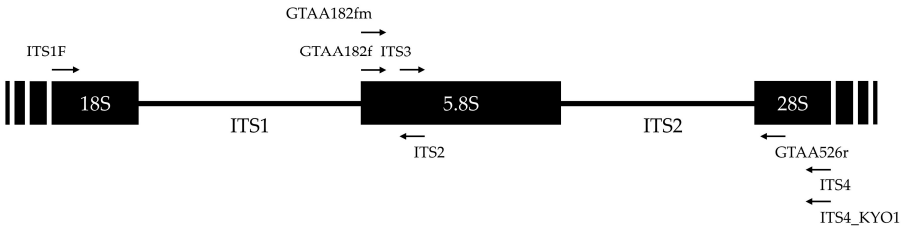

Figure 6. Schematic representation of the fixation sites of forward and reverse primers listed in Table 6 on the ITS region of *N. parvum* (OL639139.1) as an example. Forward primers are represented by right-pointing arrows, and reverse primers by left-pointing arrows.

4.2. Fungal Mock Communities

Taxonomic identity of isolates used to construct mock communities were preliminarily checked by amplifying the region targeted by the ITS4/ITS5 primer pair, following PCR conditions described in White et al. [36]. Sanger sequencing of amplicons was performed by Eurofins Genomics platform (Cologne, Germany). Contig assembly and taxonomic assignment were performed with Geneious Prime 2021.1.1.

Five mock communities (Mock1–Mock5) were generated by combining DNA solutions in equal concentrations from pure cultures of walnut fungal pathogens isolated from symp-

tomatic walnut husks and twigs collected in French walnut orchards. In addition, cultures from the Westerdijk Fungal Biodiversity Institute (CBS collection, Utrecht, Netherlands) and the University of Western Brittany Culture Collection (UBOCC, Plouzané, France) were also included to cover the range of pathogenic fungal species associated with walnut decay and necrotic twigs reported in several countries (Table 7). DNA extracted from asymptomatic walnut husks was added in Mock5 to evaluate the potential matrix effect on species amplification during PCR given the high levels of potential PCR inhibitors, including polyphenols, in husks [140,141] (Table 7). Besides known walnut pathogens, mock communities were also composed of DNA from non-phytopathogenic fungi frequently isolated in symptomatic organs during preliminary tests, i.e., *Gibellulopsis nigrescens* and *Epicoccum nigrum*. Pure fungal cultures and mock communities DNA concentrations were quantified with a Quantus™ Fluorometer and a QuantiFluor® ONE ds DNA System (Promega Corporation, Madison, WI, USA). Three replicates were prepared for each mock community.

Table 7. Species included in mock communities and their origin. Each mock community was composed of DNA solutions of the same concentration in the same proportion.

Classification	Species	Strain No.	DNA Solutions Included in Mocks				
			Mock1 [e]	Mock2 [f]	Mock3 [g]	Mock4 [h]	Mock5 [i]
Plant							
Juglandaceae	*Juglans regia*	-					X
Fungi							
Botryosphaeriaceae	*Botryosphaeria dothidea*	P12N1I2_2020 [a]	X		X	X	X
	Diplodia seriata	CBS112555 [b]	X		X	X	X
	Dothiorella omnivora	CBS140349 [b]	X		X	X	X
	Lasiodiplodia theobromae	CBS164.96 [b]	X		X	X	X
	Neofusicoccum mediterraneum	CBS121718 [b]	X		X	X	X
	N. parvum	P12N1I1_2020 [a]	X		X	X	X
Diaporthaceae	*Diaporthe amygdali*	CBS126679 [b]		X	X	X	X
	Dia. eres	P12N2I3_2020 [a]		X	X	X	X
	Dia. foeniculina	UBOCC-A-122019 [c]		X	X	X	X
	Dia. novem	UBOCC-A-122020 [c]		X	X	X	X
	Dia. rudis	P9N3I1_2020 [a]		X	X	X	X
Didymellaceae	*Epicoccum nigrum*	P12N5I8_2020 [a]			X	X	X
Glomerellaceae	*Colletotrichum fioriniae*	UBOCC-A-122017 [c]			X	X	X
	C. godetiae	UBOCC-A-122016 [c]			X	X	X
Nectriaceae	*Fusarium juglandicola*	UBOCC-A-119001 [d]			X	X	X
	F. solani	UBOCC-A-122023 [c]			X	X	X
Plectosphaerellaceae	*Gibellulopsis nigrescens*	UBOCC-A-122024 [c]				X	
Pleosporaceae	*Alternaria alternata*	UBOCC-A-122015 [c]			X	X	X

[a] Strains isolated from environmental samples and long-time conserved in 20% glycerol at −80 °C at LUBEM laboratory; [b] Strains from the CBS collection; [c] Strains isolated from environmental samples and added in UBOCC for this study; [d] Strain from the UBOCC; [e] Six fungal species—equivalent to 16.67% volume each; [f] Five fungal species—equivalent to 20% volume each; [g] Seventeen fungal species—equivalent to 5.89% volume each; [h] Eighteen fungal species—equivalent to 5.56% volume each; [i] Seventeen fungal species and one plant species—equivalent to 5.56% volume each.

4.3. Sampling and Total DNA Extraction

Symptomatic walnut husks (five per orchard) and twigs (12 per orchard) from different trees were collected from three French orchards (P7, P10 and P12) located in the Southwest of France in September 2020 and May 2021, respectively. Symptoms on walnut husks were characterized by blight and necrosis, while symptomatic twigs showed necrosis and dieback symptoms. Organs were surface-sterilized as follows: 1 min in a 2% active chlorine bleach solution and 1 min in two sterile distilled water baths before drying in sterile filters. Bark of twigs was removed, and the border between healthy and necrotic tissues was cut from twigs

and walnut husks using scalpel. Then, samples were pooled by orchard and by sample type (husk or twig) before being lyophilized for 48 h (Freeze-dryer Alpha 1-4 LDplus©, Martin Christ Gefriertrocknungsanlagen GmbH, Osterode am Harz, Germany) and ground in steel jars using Retsch MM400 (Retsch GmbH, Haan, Germany) until fine powder was obtained. Environmental DNA extractions were performed in triplicate using FastDNA™ SpinKit (MP Biomedicals, Fisher Scientific, Waltham, MA, USA) following the manufacturer's instructions and quantified with a NanoDrop 1000 Spectrophotometer (Thermo Fisher Scientific, Waltham, MA, USA). To monitor potential contamination, extraction blanks were prepared alongside the samples.

4.4. Illumina MiSeq Sequencing and Sequence Analyses

Prior to sequencing, evaluation of success of PCR amplification was performed on DNA from mock communities and from walnut husks and twigs using the GTAA182f/526r, GTAA182fm/526r and ITS3/ITS4_KYO1 primer pairs. PCR stages were based on the protocol described in Morales-Cruz et al. [20] for the two initial primer pairs and in Toju et al. [38] for the latter, with a volume of 0.2 µL of DNA solution at a concentration of 20 ng/µL. All PCR were performed with a Doppio thermal cycler (VWR™) and GoTaq® G2 Flexi DNA Polymerase kit (Promega Corporation) but without BSA. The quality of the PCR products was checked using electrophoresis on 1% agarose gels with Tris-acetate-EDTA (TAE) buffer 1X (Promega Corporation) and Midori Green Advance® stain (Nippon Genetics Co. Europe GmbH, Düren, Germany). No PCR products were detected for extraction blanks.

Amplicon libraries and Illumina MiSeq PE 300 bp sequencing were performed in the same run at the McGill University and Génome Québec Innovation Center (Montréal, Canada) with same adapter FLD_ill (forward sequence: ACACTCTTTCCCTACACGACGC-TCTTCCGATCT; reverse sequence: GTGACTGGAGTTCAGACGTGTGCTCTTCCGATCT), and the PCR conditions are listed in Table S2.

Sequence analysis workflow is depicted in Figure 7. First, we used FIGARO [142] to determine optimal trimming parameters of forward and reverse reads with the best percentage of read retention [143] (estimated amplicon length set to 450 bp and minimum overlap length of 20 bases; Table S3) followed by the DADA2 R package [144] for read truncation with no ambiguous bases allowed, read denoising and filtering. Quality profiles were also inspected with DADA2 R package and reads were trimmed according to Figaro parameters allowing the inclusion of bases with a minimum Qscore of 30 (corresponding to a probability of an incorrect base call 1 in 1000 times). In the case of ITS, forward and reverse reads were non-overlapping. Therefore, optimal trimming parameters of the forward and reverse reads were assessed using FIGARO with an estimated simulated amplicon length of 450 bp without minimum overlap length (Table S3). Sequences were then concatenated by adding N bases between forward and reverse reads.

For all primer pairs, amplicon sequence variants (ASVs) were independently inferred from the forward and reverse reads of each sample using the run-specific error rates, and read pairs were merged with an overlap setting of 12 bases minimum, except for ITS reads which were concatenated using the "*justConcatenate = TRUE*" argument. Then, taxonomic assignment was performed with BLASTn command line [145] against the UNITE+INSDC non-redundant fungal ITS v9.0 database [59], and the first hit was extracted [35], and then, taxonomic assignment was manually checked and corrected by checking the first 150 hits for each ASV. In addition, a BLASTn against the ITS local database was performed for ASVs associated with species included in mock communities (details in Section 2.1). To avoid overrepresentation of rare ASVs, only those represented in at least two samples and with sequence count greater than 10 were included in community analysis [27,31,146] using the *filter_otus_from_otu_table.py* QIIME [147] script.

In order to improve taxonomic resolution, the interest of extracting ITS2 region was evaluated for both GTAAm and Kyo by adding an ITSx [68] extraction step after read merging (Figure 7).

Blank PCR samples provided by the metabarcoding sequencing platform were added to the analyses, and no sequences were detected after the pre-processing step.

Processing analyses were performed using Phyloseq R package [148]. For the alpha-diversity indexes, rarefaction was applied to normalize all datasets at the same read counts based on the smallest samples across all datasets (sample size of 18,201 reads).

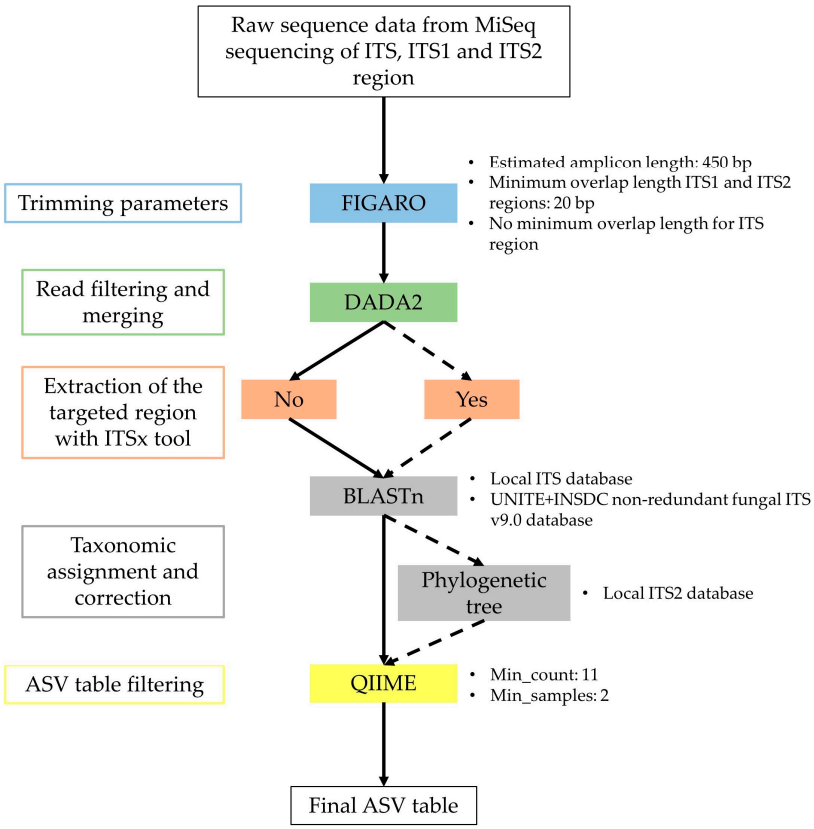

Figure 7. Workflow of bioinformatic steps and tools used in this study during data pre-processing. Parameters are listed at the right of each step. Solid arrows correspond to the basic pipeline initially followed for the five primer pairs used to sequence mock communities. Dashed arrows correspond to optional steps for GTAAm and Kyo for the sequencing of mock communities and environmental samples.

4.5. Comparative Evaluation of Primer Pairs

Four performance criteria, namely, sensitivity, precision and similarity of composition and number of ASVs were used to evaluate the performance of the five primer pairs [28]. Sensitivity was defined as the ability of a primer pair to assign well an ASV at genus level and was calculated as TP/(TP + FN), where TP corresponds to the number of true positive and FN the number of false negative ASVs (i.e., either not detected or detected but wrongly assigned at the genus level). Precision was defined as the quality of detection of fungal species and was calculated as TP/(TP + FP), where FP indicates the number of false positive ASVs (i.e., either supernumerary ASVs or ASVs assigned to unexpected genera). Similarity of composition between the recovered community and the expected community was defined as 1-BC, where BC is the Bray–Curtis similarity index and calculated as in Pauvert et al. [28]. To calculate this last criterion, taxonomic assignment obtained against the local ITS database was used. Last, the mean number of ASVs obtained for each combination of primer pair and pipeline was also determined.

4.6. Evaluation of the Taxonomic-Level Resolution

A database targeting the ITS2 region (and including 5.8S ribosomal RNA and large subunit (LSU) RNA) was constructed for GTAAm and Kyo. This local database was generated by downloading culture collection sequences from the Genbank database [73] of National Center for Biotechnology Information [74] (accessed on 17 February 2023) for each pathogenic fungal species commonly isolated from nut crops and olives (Table 5) using the query word '5.8S' with a sequence length from 200 to 5000 bp. The final database was composed of 3596 sequences for a total of 77 species. The total number of sequences per species was listed in Table S4.

To assess the taxonomic resolution of the ITS2 region targeted by GTAAm and Kyo primer pairs, phylogenetic trees were then built using this local database. First, amplicons were extracted for each primer pair following the same settings in Geneious Prime 2021.1.1, as described previously. If no amplicons were obtained in silico with these parameters, mismatches were allowed anywhere on the primer sequences (settings: pairs only anywhere on the sequences and two mismatches allowed). For each species, only unique sequences were retained by removing duplicate sequences. These selected sequences, in which taxonomic identification was manually checked using Nucleotide BLAST (https://blast.ncbi.nlm.nih.gov/Blast.cgi (accessed on 10 November 2021)), were used to build phylogenetic trees. The Kyo amplicon database contained a smaller number of species because of the difficulty in retrieving sequences long enough for reverse primer attachment. Moreover, no long enough ITS sequences of *Dothiorella omnivora* from culture collections were available to allow amplification by the two primer pairs (Table S4).

Then, final databases were aligned using MAFFT version 7 online service [149] with the Auto algorithm for alignment strategy. The resulting alignments were edited using Gblocks 0.91b [150,151] with all the options to allow less stringent selection. To evaluate the effect of ITS region extraction on primer pair resolution, the ITS2 region was extracted from amplicons of GTAAm and Kyo using ITSx [68], and phylogenetic trees were built based on extracted or non-extracted local databases. Phylogenetic trees were then constructed based on Bayesian inference with the Bayesian Evolutionary Analysis Sampling Trees 2 (BEAST2) version 2.6.1 package [152]. The best models were estimated for each amplicon database using the bModelTest add-on in Bayesian Evolutionary Analysis Utility (BEAUti2) simultaneously with the Bayesian inference analysis [153]. The analysis was performed using the Markov Chain Monte Carlo (MCMC) method by performing seven independent repetitions of 100,000,000 generations, and each sampling a tree at every 1000 generations.

Convergence of the independent Bayesian inference analyses was checked using Tracer v1.7.1 software [154] and the obtained files were combined with the LogCombiner program (frequency of resampling of 100,000 and burn-in fixed at 10%). Posterior probabilities of consensus trees were determined using the Treeannotator program and visualized using FigTree v1.4.4 [155].

Finally, taxonomic placement of ASVs from mock communities and environmental samples was checked using phylogenetic reconstructions performed following the same steps after adding the ASVs sequences to the local databases.

4.7. Statistical Analyses

Kruskal–Wallis test followed by Dunn's test were used to compare performance criteria obtained with the different primer sets and to evaluate the interest of ITSx extraction at the genus and the species level for each primer pair. Wilcoxon test without *p*-value correction was used to compare similarity of composition values between the two ITS2 region targeting primer pairs (GTAAm and Kyo) for each mock community. Expected and recovered relative abundances were calculated at the genus level by dividing the expected and recovered abundances by the total abundance obtained for each replicate. Simple linear regression between recovered and expected relative abundances were determined and Pearson correlation coefficient (R) and *p*-value were calculated. Alpha-diversity indices,

after rarefaction based on the lowest number of reads (see Section 4.4) were compared using Wilcoxon test without *p*-value correction.

5. Conclusions

In conclusion, these results indicate that targeted barcode and primer pairs greatly differ in their ability and accuracy to assess the relative abundance of fungi in a metabarcoding-sequenced community. This study provided recommendations on bioinformatic analyses and primer performance for metabarcoding sequencing of environmental samples of walnut and other nut and olive trees. Depending on the targeted species, the desired taxonomic resolution (at the genus or species level) and the scale within fungal communities (the pathobiome or the phytomicrobiome), the two GTAAm and Kyo primer sets associated with the DADA2 tool and the ITSx software are good candidates. Further work could involve a metabarcoding sequencing of other environmental samples from walnut trees to better characterize fungal communities and particularly pathobiome among different locations and assess the interactions between these fungi and the associated phytomicrobiome. Although our study was tailored for walnut samples, it could certainly be applied to almond, pistachio and olive trees and also any plant samples contaminated by these pathogens provided that local database is enriched with the plant-associated fungi of interest that were not included here.

Supplementary Materials: The following supporting information can be downloaded at: https://www.mdpi.com/article/10.3390/plants12122383/s1. Figure S1: Rarefaction curves of high-quality sequence reads for each mock community replicate. A: ITS primer set. B: ITS1 primer set. C: GTAA primer set. D: GTAAm primer set. D: Kyo primer set; Table S1: Amplification conditions for metabarcoding sequencing. Conditions are common to all primer sets. Final volume of reaction was 25 µL. Conditions were determined by Génome Québec Innovation Center; Table S2: Optimal trimming parameters of mock and environmental samples indicated by FIGARO for each primer pair; Table S3: Number of sequences for each species composing our local ITS2 database. The total number of sequences corresponds to the sequences retrieved from the Genbank database. Number of GTAAm and Kyo amplicons are the in silico amplicons obtained with the GTAA182fm/526r and ITS3/ITS4_KYO1 primer pairs. A total of 55 species and 71 species were represented in Kyo and GTAAm final databases respectively; Table S4: Total number of sequence reads obtained for each primer set and each mock replicate (−1, −2, −3) after read pre-processing step with and without the ITS2 region extraction additional step.

Author Contributions: F.P., A.P. and G.L.F. acquired funding and supervised the scientific management of the PhD work. M.B., F.P., A.P. and G.L.F. analyzed the datasets. J.-L.J. provided valuable information on phylogenetic analyses. M.B. performed sampling, metabarcoding and phylogenetic analyses and generated all tables and figures. M.B. wrote the manuscript in collaboration with A.P. and F.P. All authors have read and agreed to the published version of the manuscript.

Funding: PhD fellowship of M.B. is financed by the French Brittany region (ARED Grant #1797 SHERWOOD project) and the French ministry of Higher Education, Research and Innovation (2020 CDE EGAAL). This project was also supported by the French ministry of Agriculture and Food under CASDAR funds (AAP RT 2020 CARIBOU project coordinated by the CTIFL).

Data Availability Statement: The data presented in this study have been deposited at the NCBI and are openly available under the Bioproject PRJNA951625.

Acknowledgments: We would like to thank Cyrielle Masson (SENuRA, Isère, France) and Marie-Neige Hébrard (Walnut experimental station of Creysse, Lot, France) for sampling and sending us the environmental samples from walnut orchards as well as for their expertise in walnut dieback symptoms. We are also thankful to Agnès Verhaeghe (CTIFL) for her expertise in walnut cultures and to Yohana Laloum (CTIFL, Lanxade, France) for coordinating the CARIBOU project.

Conflicts of Interest: The authors declare no conflict of interest.

References

1. FAOSTAT Statistical Database—Production. License: CC BY-NC-SA 3.0 IGO. Available online: https://www.fao.org/faostat/en/#data/QCL (accessed on 1 February 2023).
2. Radix, P.; Seigle-Murandi, F.; Charlot, G. Walnut Blight: Development of Fruit Infection in Two Orchards. *Crop. Prot.* **1994**, *13*, 629–631. [CrossRef]
3. Yabaneri, C.; Sevim, A. Endophytic Fungi from the Common Walnut and Their in Vitro Antagonistic Activity against *Ophiognomonia leptostyla*. *Biologia* **2023**, *78*, 361–371. [CrossRef]
4. Daniels, D.A.; Nix, K.A.; Wadl, P.A.; Vito, L.M.; Wiggins, G.J.; Windham, M.T.; Ownley, B.H.; Lambdin, P.L.; Grant, J.F.; Merten, P.; et al. Thousand Cankers Disease Complex: A Forest Health Issue That Threatens *Juglans* Species across the U.S. *Forests* **2016**, *7*, 260. [CrossRef]
5. Da Lio, D.; Cobo-Díaz, J.F.; Masson, C.; Chalopin, M.; Kebe, D.; Giraud, M.; Verhaeghe, A.; Nodet, P.; Sarrocco, S.; Le Floch, G.; et al. Combined Metabarcoding and Multi-Locus Approach for Genetic Characterization of *Colletotrichum* Species Associated with Common Walnut (*Juglans regia*) Anthracnose in France. *Sci. Rep.* **2018**, *8*, 10765. [CrossRef] [PubMed]
6. Moral, J.; Morgan, D.; Trapero, A.; Michailides, T.J. Ecology and Epidemiology of Diseases of Nut Crops and Olives Caused by *Botryosphaeriaceae* Fungi in California and Spain. *Plant Dis.* **2019**, *103*, 1809–1827. [CrossRef] [PubMed]
7. López-Moral, A.; Lovera, M.; Raya, M.D.C.; Cortés-Cosano, N.; Arquero, O.; Trapero, A.; Agustí-Brisach, C. Etiology of Branch Dieback and Shoot Blight of English Walnut Caused by *Botryosphaeriaceae* and *Diaporthe* Species in Southern Spain. *Plant Dis.* **2020**, *104*, 533–550. [CrossRef]
8. Gusella, G.; Giambra, S.; Conigliaro, G.; Burruano, S.; Polizzi, G. *Botryosphaeriaceae* Species Causing Canker and Dieback of English Walnut (*Juglans regia*) in Italy. *For. Path.* **2021**, *51*, e12661. [CrossRef]
9. Yildiz, A.; Benlioglu, S.; Benlioglu, K.; Korkom, Y. Occurrence of Twig Blight and Branch Dieback of Walnut Caused by *Botryosphaeriaceae* Species in Turkey. *J. Plant Dis. Prot.* **2022**, *129*, 687–693. [CrossRef]
10. Eichmeier, A.; Pecenka, J.; Spetik, M.; Necas, T.; Ondrasek, I.; Armengol, J.; León, M.; Berlanas, C.; Gramaje, D. Fungal Trunk Pathogens Associated with *Juglans regia* in the Czech Republic. *Plant Dis.* **2020**, *104*, 761–771. [CrossRef]
11. Laloum, Y.; Verhaeghe, A.; Moronvalle, A.; Masson, C.; Hebrard, M.-N.; Picot, A.; Pensec, F.; Belair, M. Projet CARIBOU: Élancer la recherche pour cerner le dépérissement du noyer. *Infos. Ctifl.* **2022**, *386*, 48–58.
12. Moral, J.; Muñoz-Díez, C.; González, N.; Trapero, A.; Michailides, T.J. Characterization and Pathogenicity of *Botryosphaeriaceae* Species Collected from Olive and Other Hosts in Spain and California. *Phytopathology* **2010**, *100*, 1340–1351. [CrossRef]
13. Michailides, T.J.; Chen, S.; Morgan, D.; Felts, D.; Nouri, M.T.; Puckett, R.; Luna, M.; Hasey, J.; Anderson, K.; Coates, W.; et al. *Managing Botryosphaeria/Phomopsis Cankers and Anthracnose Blight of Walnut in California*; Walnut Research Reports; California Walnut Board: Folsom, CA, USA, 2013; pp. 325–346.
14. Azevedo-Nogueira, F.; Rego, C.; Gonçalves, H.M.R.; Fortes, A.M.; Gramaje, D.; Martins-Lopes, P. The Road to Molecular Identification and Detection of Fungal Grapevine Trunk Diseases. *Front. Plant Sci.* **2022**, *13*, 960289. [CrossRef]
15. Bass, D.; Stentiford, G.D.; Wang, H.-C.; Koskella, B.; Tyler, C.R. The Pathobiome in Animal and Plant Diseases. *Trends Ecol. Evol.* **2019**, *34*, 996–1008. [CrossRef]
16. Abdelfattah, A.; Malacrinò, A.; Wisniewski, M.; Cacciola, S.O.; Schena, L. Metabarcoding: A Powerful Tool to Investigate Microbial Communities and Shape Future Plant Protection Strategies. *Biol. Control.* **2018**, *120*, 1–10. [CrossRef]
17. Agler, M.T.; Ruhe, J.; Kroll, S.; Morhenn, C.; Kim, S.-T.; Weigel, D.; Kemen, E.M. Microbial Hub Taxa Link Host and Abiotic Factors to Plant Microbiome Variation. *PLoS Biol.* **2016**, *14*, e1002352. [CrossRef]
18. Busby, P.E.; Peay, K.G.; Newcombe, G. Common Foliar Fungi of *Populus Trichocarpa* Modify *Melampsora* Rust Disease Severity. *New Phytol.* **2016**, *209*, 1681–1692. [CrossRef]
19. Cobo-Díaz, J.F.; Baroncelli, R.; Le Floch, G.; Picot, A. A Novel Metabarcoding Approach to Investigate *Fusarium* Species Composition in Soil and Plant Samples. *FEMS Microbiol. Ecol.* **2019**, *95*, fiz084. [CrossRef] [PubMed]
20. Morales-Cruz, A.; Figueroa-Balderas, R.; García, J.F.; Tran, E.; Rolshausen, P.E.; Baumgartner, K.; Cantu, D. Profiling Grapevine Trunk Pathogens *in Planta*: A Case for Community-Targeted DNA Metabarcoding. *BMC Microbiol.* **2018**, *18*, 214. [CrossRef] [PubMed]
21. Cobo-Díaz, J.F.; Baroncelli, R.; Le Floch, G.; Picot, A. Combined Metabarcoding and Co-Occurrence Network Analysis to Profile the Bacterial, Fungal and *Fusarium* Communities and Their Interactions in Maize Stalks. *Front. Microbiol.* **2019**, *10*, 261. [CrossRef] [PubMed]
22. Ruppert, K.M.; Kline, R.J.; Rahman, M.S. Past, Present, and Future Perspectives of Environmental DNA (EDNA) Metabarcoding: A Systematic Review in Methods, Monitoring, and Applications of Global EDNA. *Glob. Ecol. Conserv.* **2019**, *17*, e00547. [CrossRef]
23. Vanga, B.R.; Panda, P.; Shah, A.S.; Thompson, S.; Woolley, R.H.; Ridgway, H.J.; Mundy, D.C.; Bulman, S. DNA Metabarcoding Reveals High Relative Abundance of Trunk Disease Fungi in Grapevines from Marlborough, New Zealand. *BMC Microbiol.* **2022**, *22*, 126. [CrossRef]
24. Chi, W.-C.; Chen, W.; He, C.-C.; Guo, S.-Y.; Cha, H.-J.; Tsang, L.M.; Ho, T.W.; Pang, K.-L. A Highly Diverse Fungal Community Associated with Leaves of the Mangrove Plant *Acanthus Ilicifolius* var. *Xiamenensis* Revealed by Isolation and Metabarcoding Analyses. *PeerJ* **2019**, *7*, e7293. [CrossRef]

25. Wang, S.; Tan, Y.; Li, S.; Zhu, T. Structural and Dynamic Analysis of Leaf-Associated Fungal Community of Walnut Leaves Infected by Leaf Spot Disease Based Illumina High-Throughput Sequencing Technology. *Pol. J. Microbiol.* **2022**, *71*, 429–441. [CrossRef]
26. Nilsson, R.H.; Anslan, S.; Bahram, M.; Wurzbacher, C.; Baldrian, P.; Tedersoo, L. Mycobiome Diversity: High-Throughput Sequencing and Identification of Fungi. *Nat. Rev. Microbiol.* **2019**, *17*, 95–109. [CrossRef]
27. Alberdi, A.; Aizpurua, O.; Gilbert, M.T.P.; Bohmann, K. Scrutinizing Key Steps for Reliable Metabarcoding of Environmental Samples. *Methods Ecol. Evol.* **2018**, *9*, 134–147. [CrossRef]
28. Pauvert, C.; Buée, M.; Laval, V.; Edel-Hermann, V.; Fauchery, L.; Gautier, A.; Lesur, I.; Vallance, J.; Vacher, C. Bioinformatics Matters: The Accuracy of Plant and Soil Fungal Community Data Is Highly Dependent on the Metabarcoding Pipeline. *Fungal Ecol.* **2019**, *41*, 23–33. [CrossRef]
29. Tedersoo, L.; Lindahl, B. Fungal Identification Biases in Microbiome Projects. *Environ. Microbiol. Rep.* **2016**, *8*, 774–779. [CrossRef]
30. Nichols, R.V.; Vollmers, C.; Newsom, L.A.; Wang, Y.; Heintzman, P.D.; Leighton, M.; Green, R.E.; Shapiro, B. Minimizing Polymerase Biases in Metabarcoding. *Mol. Ecol. Resour.* **2018**, *18*, 927–939. [CrossRef] [PubMed]
31. Oliver, A.K.; Brown, S.P.; Callaham, M.A.; Jumpponen, A. Polymerase Matters: Non-Proofreading Enzymes Inflate Fungal Community Richness Estimates by up to 15%. *Fungal Ecol.* **2015**, *15*, 86–89. [CrossRef]
32. Smith, D.P.; Peay, K.G. Sequence Depth, Not PCR Replication, Improves Ecological Inference from Next Generation DNA Sequencing. *PLoS ONE* **2014**, *9*, e90234. [CrossRef]
33. Estensmo, E.L.F.; Maurice, S.; Morgado, L.; Martin-Sanchez, P.M.; Skrede, I.; Kauserud, H. The Influence of Intraspecific Sequence Variation during DNA Metabarcoding: A Case Study of Eleven Fungal Species. *Mol. Ecol. Resour.* **2021**, *21*, 1141–1148. [CrossRef]
34. Bazinet, A.L.; Cummings, M.P. A Comparative Evaluation of Sequence Classification Programs. *BMC Bioinform.* **2012**, *13*, 92. [CrossRef] [PubMed]
35. Schoch, C.L.; Seifert, K.A.; Huhndorf, S.; Robert, V.; Spouge, J.L.; Levesque, C.A.; Chen, W.; Fungal Barcoding Consortium; Fungal Barcoding Consortium Author List; Bolchacova, E.; et al. Nuclear Ribosomal Internal Transcribed Spacer (ITS) Region as a Universal DNA Barcode Marker for Fungi. *Proc. Natl. Acad. Sci. USA* **2012**, *109*, 6241–6246. [CrossRef] [PubMed]
36. White, T.J.; Bruns, T.; Lee, S.; Taylor, J. Amplification and Direct Sequencing of Fungal Ribosomal RNA Genes for Phylogenetics. In *PCR Protocols: A Guide to Methods and Amplifications*; Academic Press: Cambridge, MA, USA, 1990; pp. 315–322, ISBN 978-0-12-372180-8.
37. Gardes, M.; Bruns, T.D. ITS Primers with Enhanced Specificity for Basidiomycetes—Application to the Identification of Mycorrhizae and Rusts. *Mol. Ecol.* **1993**, *2*, 113–118. [CrossRef] [PubMed]
38. Toju, H.; Tanabe, A.S.; Yamamoto, S.; Sato, H. High-Coverage ITS Primers for the DNA-Based Identification of Ascomycetes and Basidiomycetes in Environmental Samples. *PLoS ONE* **2012**, *7*, e40863. [CrossRef]
39. Turenne, C.Y.; Sanche, S.E.; Hoban, D.J.; Karlowsky, J.A.; Kabani, A.M. Rapid Identification of Fungi by Using the ITS2 Genetic Region and an Automated Fluorescent Capillary Electrophoresis System. *J. Clin. Microbiol.* **1999**, *37*, 1846–1851. [CrossRef]
40. Vancov, T.; Keen, B. Amplification of Soil Fungal Community DNA Using the ITS86F and ITS4 Primers. *FEMS Microbiol. Lett.* **2009**, *296*, 91–96. [CrossRef]
41. Larena, I.; Salazar, O.; González, V.; Julián, M.C.; Rubio, V. Design of a Primer for Ribosomal DNA Internal Transcribed Spacer with Enhanced Specificity for Ascomycetes. *J. Biotechnol.* **1999**, *75*, 187–194. [CrossRef]
42. Ihrmark, K.; Bödeker, I.T.M.; Cruz-Martinez, K.; Friberg, H.; Kubartova, A.; Schenck, J.; Strid, Y.; Stenlid, J.; Brandström-Durling, M.; Clemmensen, K.E.; et al. New Primers to Amplify the Fungal ITS2 Region—Evaluation by 454-Sequencing of Artificial and Natural Communities. *FEMS Microbiol. Ecol.* **2012**, *82*, 666–677. [CrossRef]
43. Oja, J.; Kohout, P.; Tedersoo, L.; Kull, T.; Kõljalg, U. Temporal Patterns of Orchid Mycorrhizal Fungi in Meadows and Forests as Revealed by 454 Pyrosequencing. *New Phytol.* **2015**, *205*, 1608–1618. [CrossRef]
44. Tedersoo, L.; Bahram, M.; Põlme, S.; Kõljalg, U.; Yorou, N.S.; Wijesundera, R.; Ruiz, L.V.; Vasco-Palacios, A.M.; Thu, P.Q.; Suija, A.; et al. Global Diversity and Geography of Soil Fungi. *Science* **2014**, *346*, 1256688. [CrossRef] [PubMed]
45. Taylor, D.L.; Walters, W.A.; Lennon, N.J.; Bochicchio, J.; Krohn, A.; Caporaso, J.G.; Pennanen, T. Accurate Estimation of Fungal Diversity and Abundance through Improved Lineage-Specific Primers Optimized for Illumina Amplicon Sequencing. *Appl. Environ. Microbiol.* **2016**, *82*, 7217–7226. [CrossRef] [PubMed]
46. Nguyen, N.H.; Smith, D.; Peay, K.; Kennedy, P. Parsing Ecological Signal from Noise in next Generation Amplicon Sequencing. *New Phytol.* **2015**, *205*, 1389–1393. [CrossRef] [PubMed]
47. Bakker, M.G. A Fungal Mock Community Control for Amplicon Sequencing Experiments. *Mol. Ecol. Resour.* **2018**, *18*, 541–556. [CrossRef] [PubMed]
48. Yamamoto, N.; Bibby, K. Clustering of Fungal Community Internal Transcribed Spacer Sequence Data Obscures Taxonomic Diversity: Taxonomic Impacts of Clustering Fungal ITS. *Environ. Microbiol.* **2014**, *16*, 2491–2500. [CrossRef]
49. Bjørnsgaard Aas, A.; Davey, M.L.; Kauserud, H. ITS All Right Mama: Investigating the Formation of Chimeric Sequences in the ITS2 Region by DNA Metabarcoding Analyses of Fungal Mock Communities of Different Complexities. *Mol. Ecol. Resour.* **2017**, *17*, 730–741. [CrossRef]
50. Op De Beeck, M.; Lievens, B.; Busschaert, P.; Declerck, S.; Vangronsveld, J.; Colpaert, J.V. Comparison and Validation of Some ITS Primer Pairs Useful for Fungal Metabarcoding Studies. *PLoS ONE* **2014**, *9*, e97629. [CrossRef]

51. Tedersoo, L.; Bahram, M.; Zinger, L.; Nilsson, R.H.; Kennedy, P.G.; Yang, T.; Anslan, S.; Mikryukov, V. Best Practices in Metabarcoding of Fungi: From Experimental Design to Results. *Mol. Ecol.* **2022**, *31*, 2769–2795. [CrossRef]
52. Větrovský, T.; Kolařík, M.; Žifčáková, L.; Zelenka, T.; Baldrian, P. The Rpb2 Gene Represents a Viable Alternative Molecular Marker for the Analysis of Environmental Fungal Communities. *Mol. Ecol. Resour.* **2016**, *16*, 388–401. [CrossRef]
53. Lücking, R.; Aime, M.C.; Robbertse, B.; Miller, A.N.; Ariyawansa, H.A.; Aoki, T.; Cardinali, G.; Crous, P.W.; Druzhinina, I.S.; Geiser, D.M.; et al. Unambiguous Identification of Fungi: Where Do We Stand and How Accurate and Precise Is Fungal DNA Barcoding? *IMA Fungus* **2020**, *11*, 14. [CrossRef]
54. Bokulich, N.A.; Mills, D.A. Improved Selection of Internal Transcribed Spacer-Specific Primers Enables Quantitative, Ultra-High-Throughput Profiling of Fungal Communities. *Appl. Environ. Microbiol.* **2013**, *79*, 2519–2526. [CrossRef] [PubMed]
55. Yang, R.-H.; Su, J.-H.; Shang, J.-J.; Wu, Y.-Y.; Li, Y.; Bao, D.-P.; Yao, Y.-J. Evaluation of the Ribosomal DNA Internal Transcribed Spacer (ITS), Specifically ITS1 and ITS2, for the Analysis of Fungal Diversity by Deep Sequencing. *PLoS ONE* **2018**, *13*, e0206428. [CrossRef] [PubMed]
56. Blaalid, R.; Kumar, S.; Nilsson, R.H.; Abarenkov, K.; Kirk, P.M.; Kauserud, H. ITS1 versus ITS2 as DNA Metabarcodes for Fungi. *Mol. Ecol. Resour.* **2013**, *13*, 218–224. [CrossRef] [PubMed]
57. Wang, X.-C.; Liu, C.; Huang, L.; Bengtsson-Palme, J.; Chen, H.; Zhang, J.-H.; Cai, D.; Li, J.-Q. ITS1: A DNA Barcode Better than ITS2 in Eukaryotes? *Mol. Ecol. Resour.* **2015**, *15*, 573–586. [CrossRef] [PubMed]
58. Bazzicalupo, A.L.; Bálint, M.; Schmitt, I. Comparison of ITS1 and ITS2 RDNA in 454 Sequencing of Hyperdiverse Fungal Communities. *Fungal Ecol.* **2013**, *6*, 102–109. [CrossRef]
59. Nilsson, R.H.; Larsson, K.-H.; Taylor, A.F.S.; Bengtsson-Palme, J.; Jeppesen, T.S.; Schigel, D.; Kennedy, P.; Picard, K.; Glöckner, F.O.; Tedersoo, L.; et al. The UNITE Database for Molecular Identification of Fungi: Handling Dark Taxa and Parallel Taxonomic Classifications. *Nucleic Acids Res.* **2019**, *47*, D259–D264. [CrossRef]
60. del Campo, J.; Kolisko, M.; Boscaro, V.; Santoferrara, L.; Nenarokov, S.; Massana, R.; Guillou, L.; Simpson, A.; Berney, C.; de Vargas, C.; et al. EukRef: Phylogenetic Curation of Ribosomal RNA to Enhance Understanding of Eukaryotic Diversity and Distribution. *PLoS Biol.* **2018**, *16*, e2005849. [CrossRef] [PubMed]
61. Arranz, V.; Pearman, W.S.; Aguirre, J.D.; Liggins, L. MARES, a Replicable Pipeline and Curated Reference Database for Marine Eukaryote Metabarcoding. *Sci. Data* **2020**, *7*, 209. [CrossRef]
62. Porter, T.M.; Hajibabaei, M. Putting COI Metabarcoding in Context: The Utility of Exact Sequence Variants (ESVs) in Biodiversity Analysis. *Front. Ecol. Evol.* **2020**, *8*, 248. [CrossRef]
63. Rué, O.; Coton, M.; Dugat-Bony, E.; Howell, K.; Irlinger, F.; Legras, J.-L.; Loux, V.; Michel, E.; Mounier, J.; Neuvéglise, C.; et al. Comparison of Metabarcoding Taxonomic Markers to Describe Fungal Communities in Fermented Foods. *bioRxiv* **2023**. bioRxiv:13.523754. [CrossRef]
64. Tedersoo, L.; Anslan, S.; Bahram, M.; Põlme, S.; Riit, T.; Liiv, I.; Kõljalg, U.; Kisand, V.; Nilsson, H.; Hildebrand, F.; et al. Shotgun Metagenomes and Multiple Primer Pair-Barcode Combinations of Amplicons Reveal Biases in Metabarcoding Analyses of Fungi. *MycoKeys* **2015**, *10*, 1–43. [CrossRef]
65. Ehrich, M.; Zoll, S.; Sur, S.; van den Boom, D. A New Method for Accurate Assessment of DNA Quality after Bisulfite Treatment. *Nucleic Acids Res.* **2007**, *35*, e29. [CrossRef] [PubMed]
66. Edwards, J.E.; Hermes, G.D.A.; Kittelmann, S.; Nijsse, B.; Smidt, H. Assessment of the Accuracy of High-Throughput Sequencing of the ITS1 Region of *Neocallimastigomycota* for Community Composition Analysis. *Front. Microbiol.* **2019**, *10*, 2370. [CrossRef] [PubMed]
67. Lofgren, L.A.; Uehling, J.K.; Branco, S.; Bruns, T.D.; Martin, F.; Kennedy, P.G. Genome-based Estimates of Fungal RDNA Copy Number Variation across Phylogenetic Scales and Ecological Lifestyles. *Mol. Ecol.* **2019**, *28*, 721–730. [CrossRef] [PubMed]
68. Bengtsson-Palme, J.; Ryberg, M.; Hartmann, M.; Branco, S.; Wang, Z.; Godhe, A.; De Wit, P.; Sánchez-García, M.; Ebersberger, I.; de Sousa, F.; et al. Improved Software Detection and Extraction of ITS1 and ITS2 from Ribosomal ITS Sequences of *Fungi* and Other Eukaryotes for Analysis of Environmental Sequencing Data. *Methods Ecol. Evol.* **2013**, *4*, 914–919. [CrossRef]
69. Tedersoo, L.; Drenkhan, R.; Anslan, S.; Morales-Rodriguez, C.; Cleary, M. High-Throughput Identification and Diagnostics of Pathogens and Pests: Overview and Practical Recommendations. *Mol. Ecol.* **2018**, *19*, 47–76. [CrossRef]
70. Sohrabi, M.; Mohammadi, H.; León, M.; Armengol, J.; Banihashemi, Z. Fungal Pathogens Associated with Branch and Trunk Cankers of Nut Crops in Iran. *Eur. J. Plant Pathol.* **2020**, *157*, 327–351. [CrossRef]
71. Voglmayr, H.; Castlebury, L.A.; Jaklitsch, W.M. *Juglanconis* Gen. Nov. on *Juglandaceae*, and the New Family *Juglanconidaceae* (*Diaporthales*). *Persoonia* **2017**, *38*, 136–155. [CrossRef]
72. Belisario, A. Cultural Characteristics and Pathogenicity of *Melanconium juglandinum*. *Eur. J. For. Pathol.* **1999**, *29*, 317–322. [CrossRef]
73. Sayers, E.W.; Cavanaugh, M.; Clark, K.; Pruitt, K.D.; Schoch, C.L.; Sherry, S.T.; Karsch-Mizrachi, I. GenBank. *Nucleic Acids Res.* **2022**, *50*, D161–D164. [CrossRef]
74. National Center for Biotechnology Information. Available online: https://www.ncbi.nlm.nih.gov/ (accessed on 21 May 2021).
75. O'Leary, N.A.; Wright, M.W.; Brister, J.R.; Ciufo, S.; Haddad, D.; McVeigh, R.; Rajput, B.; Robbertse, B.; Smith-White, B.; Ako-Adjei, D.; et al. Reference Sequence (RefSeq) Database at NCBI: Current Status, Taxonomic Expansion, and Functional Annotation. *Nucleic Acids Res.* **2016**, *44*, D733–D745. [CrossRef]

76. Kolařík, M.; Hulcr, J.; Tisserat, N.; De Beer, W.; Kostovčík, M.; Kolaříková, Z.; Seybold, S.J.; Rizzo, D.M. *Geosmithia* Associated with Bark Beetles and Woodborers in the Western USA: Taxonomic Diversity and Vector Specificity. *Mycologia* **2017**, *109*, 185–199. [CrossRef]
77. Montecchio, L.; Fanchin, G.; Simonato, M.; Faccoli, M. First Record of Thousand Cankers Disease Fungal Pathogen *Geosmithia Morbida* and Walnut Twig Beetle *Pityophthorus Juglandis* on *Juglans regia* in Europe. *Plant Dis.* **2014**, *98*, 1445. [CrossRef]
78. Yaghmour, M.A.; Nguyen, T.L.; Roubtsova, T.V.; Hasey, J.K.; Fichtner, E.J.; DeBuse, C.; Seybold, S.J.; Bostock, R.M. First Report of *Geosmithia Morbida* on English Walnut and Its Paradox Rootstock in California. *Plant Dis.* **2014**, *98*, 1441. [CrossRef]
79. Zhu, Y.F.; Yin, Y.F.; Qu, W.W.; Yang, K.Q. Occurence and Spread of the Pathogens on Walnut (*Juglans regia*) in Shandong Province, China. In *ISHS Acta Horticulturae 1050: VII International Walnut Symposium*; ISHS: Leuven, Belgium, 2014; pp. 347–351. [CrossRef]
80. Chen, S.F.; Morgan, D.P.; Hasey, J.K.; Anderson, K.; Michailides, T.J. Phylogeny, Morphology, Distribution, and Pathogenicity of *Botryosphaeriaceae* and *Diaporthaceae* from English Walnut in California. *Plant Dis.* **2014**, *98*, 636–652. [CrossRef]
81. Inderbitzin, P.; Bostock, R.M.; Trouillas, F.P.; Michailides, T.J. A Six Locus Phylogeny Reveals High Species Diversity in *Botryosphaeriaceae* from California Almond. *Mycologia* **2010**, *102*, 1350–1368. [CrossRef]
82. Gramaje, D.; Agustí-Brisach, C.; Pérez-Sierra, A.; Moralejo, E.; Olmo, D.; Mostert, L.; Damm, U.; Armengol, J. Fungal Trunk Pathogens Associated with Wood Decay of Almond Trees on Mallorca (Spain). *Persoonia* **2012**, *28*, 1–13. [CrossRef]
83. Úrbez-Torres, J.R.; Peduto, F.; Vossen, P.M.; Krueger, W.H.; Gubler, W.D. Olive Twig and Branch Dieback: Etiology, Incidence, and Distribution in California. *Plant Dis.* **2013**, *97*, 231–244. [CrossRef] [PubMed]
84. Carlucci, A.; Raimondo, M.L.; Cibelli, F.; Phillips, A.J.L.; Lops, F. *Pleurostomophora Richardsiae*, *Neofusicoccum Parvum* and *Phaeoacremonium Aleophilum* Associated with a Decline of Olives in Southern Italy. *Phytopathol. Mediterr.* **2013**, *52*, 517–527.
85. López-Moral, A.; del Carmen Raya, M.; Ruiz-Blancas, C.; Medialdea, I.; Lovera, M.; Arquero, O.; Trapero, A.; Agustí-Brisach, C. Aetiology of Branch Dieback, Panicle and Shoot Blight of Pistachio Associated with Fungal Trunk Pathogens in Southern Spain. *Plant Pathol.* **2020**, *69*, 1237–1269. [CrossRef]
86. Jiménez Luna, I.; Besoain, X.; Saa, S.; Peach-Fine, E.; Morales, F.C.; Riquelme, N.; Larach, A.; Morales, J.; Ezcurra, E.; Ashworth, V.E.T.M.; et al. Identity and Pathogenicity of *Botryosphaeriaceae* and *Diaporthaceae* from *Juglans regia* in Chile. *Phytopathol. Mediterr.* **2022**, *61*, 79–94. [CrossRef]
87. Holland, L.A.; Trouillas, F.P.; Nouri, M.T.; Lawrence, D.P.; Crespo, M.; Doll, D.A.; Duncan, R.A.; Holtz, B.A.; Culumber, C.M.; Yaghmour, M.A.; et al. Fungal Pathogens Associated with Canker Diseases of Almond in California. *Plant Dis.* **2021**, *105*, 346–360. [CrossRef] [PubMed]
88. Nouri, M.T.; Lawrence, D.P.; Holland, L.A.; Doll, D.A.; Kallsen, C.E.; Culumber, C.M.; Trouillas, F.P. Identification and Pathogenicity of Fungal Species Associated with Canker Diseases of Pistachio in California. *Plant Dis.* **2019**, *103*, 2397–2411. [CrossRef] [PubMed]
89. Zhang, M.; Zhang, Y.K.; Geng, Y.H.; Zang, R.; Wu, H.Y. First Report of *Diplodia Seriata* Causing Twig Dieback of English Walnut in China. *Plant Dis.* **2017**, *101*, 1036. [CrossRef]
90. Spies, C.F.J.; Mostert, L.; Carlucci, A.; Moyo, P.; van Jaarsveld, W.J.; du Plessis, I.L.; van Dyk, M.; Halleen, F. Dieback and Decline Pathogens of Olive Trees in South Africa. *Persoonia* **2020**, *45*, 196–220. [CrossRef]
91. Chen, S.F.; Morgan, D.P.; Michailides, T.J. *Botryosphaeriaceae* and *Diaporthaceae* Associated with Panicle and Shoot Blight of Pistachio in California, USA. *Fungal Divers.* **2014**, *67*, 157–179. [CrossRef]
92. Chen, S.; Li, G.; Liu, F.; Michailides, T.J. Novel Species of *Botryosphaeriaceae* Associated with Shoot Blight of Pistachio. *Mycologia* **2015**, *107*, 780–792. [CrossRef]
93. Li, G.; Liu, F.; Li, J.; Liu, Q.; Chen, S. Characterization of *Botryosphaeria Dothidea* and *Lasiodiplodia Pseudotheobromae* from English Walnut in China. *J. Phytopathol.* **2016**, *164*, 348–353. [CrossRef]
94. Derviş, S.; Türkölmez, Ş.; Çiftçi, O.; Ulubaş Serçe, Ç.; Dikilitas, M. First Report of *Neoscytalidium Dimidiatum* Causing Canker, Shoot Blight, and Root Rot of Pistachio in Turkey. *Plant Dis.* **2019**, *103*, 1411. [CrossRef]
95. Güney, İ.G.; Özer, G.; Türkölmez, Ş.; Derviş, S. Canker and Leaf Scorch on Olive (*Olea europaea* L.) Caused by *Neoscytalidium Dimidiatum* in Turkey. *Crop. Prot.* **2022**, *157*, 105985. [CrossRef]
96. Derviş, S.; Türkölmez, Ş.; Çiftçi, O.; Ulubaş Serçe, Ç.; Dikilitas, M. First Report of *Neoscytalidium Dimidiatum* Causing Black Canker and Root Rot of Walnut in Turkey. *Plant Dis.* **2019**, *103*, 2129. [CrossRef]
97. Meng, L.; Yu, C.; Wang, C.; Li, G. First Report of *Diaporthe Amygdali* Causing Walnut Twig Canker in Shandong Province of China. *Plant Dis.* **2018**, *102*, 1859. [CrossRef]
98. Diogo, E.L.F.; Santos, J.M.; Phillips, A.J.L. Phylogeny, Morphology and Pathogenicity of *Diaporthe* and *Phomopsis* Species on Almond in Portugal. *Fungal Divers.* **2010**, *44*, 107–115. [CrossRef]
99. Yang, Q.; Fan, X.-L.; Guarnaccia, V.; Tian, C.-M. High Diversity of *Diaporthe* Species Associated with Dieback Diseases in China, with Twelve New Species Described. *MycoKeys* **2018**, *39*, 97–149. [CrossRef] [PubMed]
100. Fang, X.; Qin, K.; Li, S.; Han, S.; Zhu, T.; Fang, X.; Qin, K. Whole Genome Sequence of *Diaporthe Capsici*, a New Pathogen of Walnut Blight. *Genomics* **2020**, *112*, 3751–3761. [CrossRef] [PubMed]
101. Fan, X.; Yang, Q.; Bezerra, J.D.P.; Alvarez, L.V.; Tian, C. *Diaporthe* from Walnut Tree (*Juglans regia*) in China, with Insight of the *Diaporthe Eres* Complex. *Mycol. Prog.* **2018**, *17*, 841–853. [CrossRef]

102. Kanematsu, S.; Minaka, N.; Kobayashi, T.; Kudo, A.; Ohtsu, Y. Molecular Phylogenetic Analysis of Ribosomal DNA Internal Transcribed Spacer Regions and Comparison of Fertility in *Phomopsis* Isolates from Fruit Trees. *J. Gen. Plant Pathol.* **2000**, *66*, 191–201. [CrossRef]
103. Zhou, H.; Hou, C.-L. Three New Species of *Diaporthe* from China Based on Morphological Characters and DNA Sequence Data Analyses. *Phytotaxa* **2019**, *422*, 157–174. [CrossRef]
104. He, L.; Li, X.; Gao, Y.; Li, B.; Mu, W.; Liu, F. Characterization and Fungicide Sensitivity of *Colletotrichum* spp. from Different Hosts in Shandong, China. *Plant Dis.* **2019**, *103*, 34–43. [CrossRef]
105. de Silva, D.D.; Mann, R.C.; Kaur, J.; Ekanayake, P.N.; Sawbridge, T.I.; McKay, S.; Taylor, P.W.J.; Edwards, J. Revisiting the *Colletotrichum* Species Causing Anthracnose of Almond in Australia. *Australas. Plant Pathol.* **2021**, *50*, 267–279. [CrossRef]
106. López-Moral, A.; Raya-Ortega, M.C.; Agustí-Brisach, C.; Roca, L.F.; Lovera, M.; Luque, F.; Arquero, O.; Trapero, A. Morphological, Pathogenic, and Molecular Characterization of *Colletotrichum acutatum* Isolates Causing Almond Anthracnose in Spain. *Plant Dis.* **2017**, *101*, 2034–2045. [CrossRef]
107. Mosca, S.; Nicosia, M.G.L.D.; Cacciola, S.O.; Schena, L. Molecular Analysis of *Colletotrichum* Species in the Carposphere and Phyllosphere of Olive. *PLoS ONE* **2014**, *9*, e114031. [CrossRef] [PubMed]
108. Shivas, R.G.; Tan, Y.P.; Edwards, J.; Dinh, Q.; Maxwell, A.; Andjic, V.; Liberato, J.R.; Anderson, C.; Beasley, D.R.; Bransgrove, K.; et al. *Colletotrichum* Species in Australia. *Australas. Plant Pathol.* **2016**, *45*, 447–464. [CrossRef]
109. Wei, X.; Yang, S.Q.; Jiang, Z.G.; Cui, M.J.; Deng, J.X.; Zhang, Y. *Colletotrichum Juglandis* sp. nov. (*Ascomycota*: *Glomerellaceae*) Associated with Walnut Leaf Spot in China. *Phytotaxa* **2022**, *556*, 256–268. [CrossRef]
110. Liu, B.; Pavel, J.A.; Hausbeck, M.K.; Feng, C.; Correll, J.C. Phylogenetic Analysis, Vegetative Compatibility, Virulence, and Fungal Filtrates of Leaf Curl Pathogen *Colletotrichum Fioriniae* from Celery. *Phytopathology* **2021**, *111*, 751–760. [CrossRef] [PubMed]
111. Lichtemberg, P.S.F.; Moral, J.; Morgan, D.P.; Felts, D.G.; Sanders, R.D.; Michailides, T.J. First Report of Anthracnose Caused by *Colletotrichum Fioriniae* and *C. Karstii* in California Pistachio Orchards. *Plant Dis.* **2017**, *101*, 1320. [CrossRef]
112. Wang, Q.H.; Li, D.W.; Duan, C.H.; Liu, X.H.; Niu, S.G.; Hou, L.Q.; Wu, X.Q. First Report of Walnut Anthracnose Caused by *Colletotrichum Fructicola* in China. *Plant Dis.* **2018**, *102*, 247. [CrossRef]
113. Wang, Q.-H.; Fan, K.; Li, D.-W.; Han, C.-M.; Qu, Y.-Y.; Qi, Y.-K.; Wu, X.-Q. Identification, Virulence and Fungicide Sensitivity of *Colletotrichum Gloeosporioides s.s.* Responsible for Walnut Anthracnose Disease in China. *Plant Dis.* **2020**, *104*, 1358–1368. [CrossRef]
114. Schena, L.; Mosca, S.; Cacciola, S.O.; Faedda, R.; Sanzani, S.M.; Agosteo, G.E.; Sergeeva, V.; Magnano di San Lio, G. Species of the *Colletotrichum Gloeosporioides* and *C. Boninense* Complexes Associated with Olive Anthracnose. *Plant Pathol.* **2014**, *63*, 437–446. [CrossRef]
115. Savian, L.G.; Muniz, M.F.B.; Poletto, T.; Maculan, L.G.; Rabuske, J.E.; Blume, E.; Sarzi, J.S. First Report of *Colletotrichum Nymphaeae* Causing Anthracnose on *Juglans regia* Fruits in Southern Brazil. *Plant Dis.* **2019**, *103*, 3287. [CrossRef]
116. Varjas, V.; Szilágyi, S.; Lakatos, T. First Report of *Colletotrichum Nymphaeae* Causing Anthracnose on Almond in Hungary. *Plant Dis.* **2022**, *106*, 1527. [CrossRef]
117. Damm, U.; Cannon, P.F.; Woudenberg, J.H.C.; Crous, P.W. The *Colletotrichum acutatum* Species Complex. *Stud. Mycol.* **2012**, *73*, 37–113. [CrossRef]
118. Walker, D.M.; Castlebury, L.A.; Rossman, A.Y.; Mejía, L.C.; White, J.F. Phylogeny and Taxonomy of *Ophiognomonia* (*Gnomoniaceae*, *Diaporthales*), Including Twenty-Five New Species in This Highly Diverse Genus. *Fungal Divers.* **2012**, *57*, 85–147. [CrossRef]
119. Belisario, A.; Scotton, M.; Santori, A.; Onofri, S. Variability in the Italian Population of *Gnomonia Leptostyla*, Homothallism and Resistance of *Juglans* Species to Anthracnose. *For. Pathol.* **2008**, *38*, 129–145. [CrossRef]
120. Ma, R.; Ye, S.; Zhao, Y.; Michailides, T.J.; Tian, C. New Leaf and Fruit Disease of *Juglans regia* Caused by *Juglanconis Juglandina* in Xinjiang, China. *For. Path.* **2019**, *49*, e12537. [CrossRef]
121. Moya-Elizondo, E.A.; Lagos, M.J.; San Martin, J.; Ruiz, B. First Report of *Alternaria Alternata* and *Fusarium* spp. Causing Brown Apical Necrosis in Walnut Fruit in Southern Chile. *Plant Health Prog.* **2021**, *22*, 573–574. [CrossRef]
122. Wang, Y.X.; Chen, J.Y.; Xu, X.W.; Li, D.W.; Wang, Q.Z. First Report of Brown Apical Necrosis of Walnut Fruit Caused by *Fusarium Avenaceum* in Hubei, China. *Plant Dis.* **2019**, *103*, 2956. [CrossRef]
123. Belisario, A.; Maccaroni, M.; Corazza, L.; Balmas, V.; Valier, A. Occurrence and Etiology of Brown Apical Necrosis on Persian (English) Walnut Fruit. *Plant Dis.* **2002**, *86*, 599–602. [CrossRef] [PubMed]
124. Marek, S.M.; Yaghmour, M.A.; Bostock, R.M. *Fusarium* spp., *Cylindrocarpon* spp., and Environmental Stress in the Etiology of a Canker Disease of Cold-Stored Fruit and Nut Tree Seedlings in California. *Plant Dis.* **2013**, *97*, 259–270. [CrossRef]
125. Chen, W.; Ntahimpera, N.; Morgan, D.P.; Michailides, T.J. Mycoflora of *Pistacia Vera* in the Central Valley, California. *Mycotaxon* **2002**, *83*, 147–158.
126. Trabelsi, R.; Sellami, H.; Gharbi, Y.; Krid, S.; Cheffi, M.; Kammoun, S.; Dammak, M.; Mseddi, A.; Gdoura, R.; Triki, M.A. Morphological and Molecular Characterization of *Fusarium* spp. Associated with Olive Trees Dieback in Tunisia. *3 Biotech* **2017**, *7*, 28. [CrossRef] [PubMed]
127. Singh, B.; Kalha, C.S.; Razdan, V.K.; Verma, V.S. First Report of Walnut Canker Caused by *Fusarium Incarnatum* from India. *Plant Dis.* **2011**, *95*, 1587. [CrossRef] [PubMed]
128. Crous, P.W.; Cowan, D.A.; Maggs-Kölling, G.; Yilmaz, N.; Thangavel, R.; Wingfield, M.J.; Noordeloos, M.E.; Dima, B.; Brandrud, T.E.; Jansen, G.M.; et al. Fungal Planet Description Sheets: 1182–1283. *Persoonia* **2021**, *46*, 313. [CrossRef] [PubMed]

129. Crespo, M.; Lawrence, D.P.; Nouri, M.T.; Doll, D.A.; Trouillas, F.P. Characterization of *Fusarium* and *Neocosmospora* Species Associated With Crown Rot and Stem Canker of Pistachio Rootstocks in California. *Plant Dis.* **2019**, *103*, 1931–1939. [CrossRef] [PubMed]
130. Chen, W.; Swart, W.J. First Report of Stem Canker of English Walnut Caused by *Fusarium Solani* in South Africa. *Plant Dis.* **2000**, *84*, 592. [CrossRef] [PubMed]
131. Montecchio, L.; Faccoli, M.; Short, D.P.G.; Fanchin, G.; Geiser, D.M.; Kasson, M.T. First Report of *Fusarium Solani* Phylogenetic Species 25 Associated With Early Stages of Thousand Cankers Disease on *Juglans Nigra* and *Juglans regia* in Italy. *Plant Dis.* **2015**, *99*, 1183. [CrossRef]
132. Teviotdale, B.L.; Viveros, M.; Pryor, B.; Adaskaveg, J.E. First Report of Alternaria Leaf Spot of Almond Caused by Species in the *Alternaria Alternata* Complex in California. *Plant Dis.* **2001**, *85*, 558. [CrossRef]
133. Ozkilinc, H.; Sarpkaya, K.; Kurt, S.; Can, C.; Polatbilek, H.; Yasar, A.; Sevinc, U.; Uysal, A.; Konukoglu, F. Pathogenicity, Morpho-Species and Mating Types of *Alternaria* spp. Causing Alternaria Blight in *Pistacia* spp. in Turkey. *Phytoparasitica* **2017**, *45*, 719–728. [CrossRef]
134. Carlucci, A.; Lops, F.; Cibelli, F.; Raimondo, M.L. *Phaeoacremonium* Species Associated with Olive Wilt and Decline in Southern Italy. *Eur. J. Plant Pathol.* **2015**, *141*, 717–729. [CrossRef]
135. Raimondo, M.L.; Lops, F.; Carlucci, A. First Report of *Phaeoacremonium Oleae* and *P. Viticola* Associated with Olive Trunk Diseases in Italy. *Plant Dis.* **2021**, *106*, 331. [CrossRef]
136. Lawrence, D.P.; Holland, L.A.; Nouri, M.T.; Travadon, R.; Abramians, A.; Michailides, T.J.; Trouillas, F.P. Molecular Phylogeny of *Cytospora* Species Associated with Canker Diseases of Fruit and Nut Crops in California, with the Descriptions of Ten New Species and One New Combination. *IMA Fungus* **2018**, *9*, 333–369. [CrossRef]
137. Fan, X.L.; Bezerra, J.D.P.; Tian, C.M.; Crous, P.W. *Cytospora* (*Diaporthales*) in China. *Persoonia* **2020**, *45*, 1–45. [CrossRef]
138. Fotouhifar, K.-B.; Hedjaroude, G.-A.; Leuchtmann, A. ITS RDNA Phylogeny of Iranian Strains of *Cytospora* and Associated Teleomorphs. *Mycologia* **2010**, *102*, 1369–1382. [CrossRef] [PubMed]
139. Zhao, S.F.; Guo, K.F.; He, L.; Yiming, A. First Report of *Cytospora Nivea* Causing Cytospora Canker on Walnut (*Juglans regia* L.) in the Tianshan Mountains Region of Xinjiang, China. *Plant Dis.* **2018**, *102*, 2640. [CrossRef]
140. Schrader, C.; Schielke, A.; Ellerbroek, L.; Johne, R. PCR Inhibitors—Occurrence, Properties and Removal. *J. Appl. Microbiol.* **2012**, *113*, 1014–1026. [CrossRef] [PubMed]
141. Jahanban-Esfahlan, A.; Ostadrahimi, A.; Tabibiazar, M.; Amarowicz, R. A Comprehensive Review on the Chemical Constituents and Functional Uses of Walnut (*Juglans* spp.) Husk. *Int. J. Mol. Sci.* **2019**, *20*, 3920. [CrossRef]
142. Sasada, R.; Weinstein, M.; Prem, A.; Jin, M.; Bhasin, J. FIGARO: An Efficient and Objective Tool for Optimizing Microbiome RRNA Gene Trimming Parameters. *J. Biomol. Tech.* **2020**, *31*, S2.
143. Edgar, R.C.; Flyvbjerg, H. Error Filtering, Pair Assembly and Error Correction for Next-Generation Sequencing Reads. *Bioinformatics* **2015**, *31*, 3476–3482. [CrossRef]
144. Callahan, B.J.; McMurdie, P.J.; Rosen, M.J.; Han, A.W.; Johnson, A.J.A.; Holmes, S.P. DADA2: High Resolution Sample Inference from Illumina Amplicon Data. *Nat. Methods* **2016**, *13*, 581–583. [CrossRef]
145. Altschul, S.F.; Gish, W.; Miller, W.; Myers, E.W.; Lipman, D.J. Basic Local Alignment Search Tool. *J. Mol. Biol.* **1990**, *215*, 403–410. [CrossRef]
146. Brown, S.P.; Veach, A.M.; Rigdon-Huss, A.R.; Grond, K.; Lickteig, S.K.; Lothamer, K.; Oliver, A.K.; Jumpponen, A. Scraping the Bottom of the Barrel: Are Rare High Throughput Sequences Artifacts? *Fungal Ecol.* **2015**, *13*, 221–225. [CrossRef]
147. Caporaso, J.G.; Kuczynski, J.; Stombaugh, J.; Bittinger, K.; Bushman, F.D.; Costello, E.K.; Fierer, N.; Peña, A.G.; Goodrich, J.K.; Gordon, J.I.; et al. QIIME Allows Analysis of High-Throughput Community Sequencing Data. *Nat. Methods* **2010**, *7*, 335–336. [CrossRef] [PubMed]
148. McMurdie, P.J.; Holmes, S. Phyloseq: An R Package for Reproducible Interactive Analysis and Graphics of Microbiome Census Data. *PLoS ONE* **2013**, *8*, e61217. [CrossRef] [PubMed]
149. Katoh, K.; Rozewicki, J.; Yamada, K.D. MAFFT Online Service: Multiple Sequence Alignment, Interactive Sequence Choice and Visualization. *Brief. Bioinform.* **2019**, *20*, 1160–1166. [CrossRef]
150. Talavera, G.; Castresana, J. Improvement of Phylogenies after Removing Divergent and Ambiguously Aligned Blocks from Protein Sequence Alignments. *Syst. Biol.* **2007**, *56*, 564–577. [CrossRef]
151. Castresana, J. Selection of Conserved Blocks from Multiple Alignments for Their Use in Phylogenetic Analysis. *Mol. Biol. Evol.* **2000**, *17*, 540–552. [CrossRef]
152. Bouckaert, R.; Vaughan, T.G.; Barido-Sottani, J.; Duchêne, S.; Fourment, M.; Gavryushkina, A.; Heled, J.; Jones, G.; Kühnert, D.; Maio, N.D.; et al. BEAST 2.5: An Advanced Software Platform for Bayesian Evolutionary Analysis. *PLoS Comput. Biol.* **2019**, *15*, e1006650. [CrossRef]
153. Bouckaert, R.R.; Drummond, A.J. BModelTest: Bayesian Phylogenetic Site Model Averaging and Model Comparison. *BMC Evol. Biol.* **2017**, *17*, 42. [CrossRef]

154. Rambaut, A.; Drummond, A.J.; Xie, D.; Baele, G.; Suchard, M.A. Posterior Summarization in Bayesian Phylogenetics Using Tracer 1.7. *Syst. Biol.* **2018**, *67*, 901–904. [CrossRef]
155. Rambaut, A. FigTree. Available online: http://tree.bio.ed.ac.uk/software/figtree/ (accessed on 28 November 2022).